

1 Technical Note: Preventing CO₂ overestimation from mercuric or
2 copper (II) chloride preservation of dissolved greenhouse gases in
3 freshwater samples

4
5 François Clayer^{*}, Jan Erik Thrane¹, Kuria Ndungu¹, Andrew King¹, Peter Dörsch², Thomas Rohrlack²

6
7 ¹Norwegian Institute for Water Research (NIVA), Økernveien 94, 0579 Oslo, Norway

8
9 ²Faculty of Environmental Sciences and Natural Resource Management, Norwegian University of
10 Life Sciences, PO Box 5003, 1432 Ås, Norway

11
12 ^{*}Corresponding author(s): François Clayer (francois.clayer@niva.no)

13
14 **Abstract**

15 The determination of dissolved gases (O₂, CO₂, CH₄, N₂O, N₂) in surface waters allows to estimate
16 biological processes and greenhouse gas fluxes in aquatic ecosystems. Mercuric chloride (HgCl₂) has
17 been widely used to preserve water samples prior to gas analysis. However, alternates are needed
18 because of the environmental impacts and ~~regulation-prohibition~~ of mercury. HgCl₂ is a weak acid
19 and interferes with dissolved organic carbon (DOC). Hence, we tested the effect of HgCl₂ and two
20 substitutes (copper (II) chloride – CuCl₂ and silver nitrate – AgNO₃), as well as storage time (24h to 3
21 months) on the determination of dissolved gases in low ionic strength and high DOC lake-water from
22 a typical boreal lake. Furthermore, we investigated and predicted the effect of HgCl₂ on CO₂
23 concentrations in periodic samples from another lake experiencing pH variations (5.4–7.3) related to
24 *in situ* photosynthesis. Samples fixed with inhibitors generally showed negligible O₂ consumption.
25 However, effective preservation of dissolved CO₂, CH₄ and N₂O for up to three months prior to
26 dissolved gas analysis, was only achieved with AgNO₃. In contrast, HgCl₂ and CuCl₂ caused an initial
27 increase in CO₂ and N₂O from 24h to 3 weeks followed by a decrease from 3 weeks to 3 months. The
28 CO₂ overestimation, caused by HgCl₂-acidification and shift in the carbonate equilibrium, can be
29 calculated from predictions of chemical speciation. Errors due to CO₂ overestimation in HgCl₂-
30 preserved water, sampled from low ionic strength and high DOC freshwater that are common in the
31 northern hemisphere, could lead to an overestimation of the CO₂ diffusion efflux by a factor of >20
32 over a month, or a factor of 2 over the ice-free season. The use of HgCl₂ and CuCl₂ for freshwater
33 preservation should therefore be discontinued. Further testing of AgNO₃ preservation should be
34 performed under a large range of freshwater chemical characteristics.

Formatted: Subscript

Formatted: Subscript

Formatted: Subscript

CO₂ overestimation from HgCl₂ fixation – Clayer et al.

35

36 **Key-words:** lake, greenhouse gases, water sample preservation, mercuric chloride, metal toxicity,
37 carbon dioxide

38 **Running title:** CO₂ overestimation from HgCl₂ fixation

39 1 Introduction

40

41 The determination of dissolved gases by gas chromatography from water samples collected in the
42 field allows the estimation of biological processes in aquatic ecosystems such as photosynthesis and
43 oxic respiration (O₂, CO₂), denitrification (N₂, N₂O) and methanogenesis (CH₄). This technique is also
44 useful to test the calibration of *in-situ* sensors in long term deployment. However, the accuracy of this
45 approach largely depends on the effectiveness of sample fixation. In fact, the partial pressure of
46 these dissolved gases will continue to evolve in the water sample from the time of collection to the
47 time of analysis unless biological activity is prevented. This is an issue when field sites are far from
48 laboratory facilities, and it may be more efficient to process the when samples need to be stored in
49 large batches at until the end of the field season for more efficient processing in large batches. Hence,
50 before using a given biocide to preserve water samples, it must be ensured that it is efficient in
51 inhibiting biological activity without changing the sample's chemistry.

52 Mercuric (II) chloride (HgCl₂) has been widely used as an inhibitor of the above-mentioned biological
53 processes to preserve water samples for the determination of dissolved CO₂ in seawaters (e.g.
54 Dickson, Sabine & Christian, 2007) and several dissolved gases in natural and artificial freshwater
55 bodies (e.g. O₂, CO₂, CH₄, N₂ and/or N₂O; Guérin et al., 2006; Hessen et al., 2017; Hilgert et al.,
56 2019; Okuku et al., 2019; Schubert et al., 2012; Xiao et al., 2014; Yan et al., 2018; Yang et al., 2015)
57 because it is extremely toxic at very low concentrations compared to other reagents (e.g. Horvatić &
58 Peršić, 2007; Hassen *et al.*, 1998). Worldwide efforts have sought to reduce the use of mercury
59 because it is considered toxic to the environment and exposure can severely affect human health
60 (Chen et al., 2018). Therefore, alternative preservation techniques to HgCl₂ amendment have been
61 tested for dissolved inorganic carbon (DIC) and δ¹³C-DIC such as acidification with phosphoric acid
62 (Taipale & Sonninen, 2009) or a combination of filtration and exposure to benzalkonium chloride or
63 sodium chloride (Takahashi *et al.*, 2019). At least two studies, one also including dissolved organic
64 carbon (DOC) and δ¹³C-DOC, showed that simple filtration (and cooling), fixation (precipitation) or
65 acidification were better effective in preserving water samples than the use of toxic inhibitors,
66 including HgCl₂ (Wilson, Munizzi & Erhardt, 2020). Another solution is to sample the headspace out
67 in the field, and bring back gas samples (e.g., Cole et al., 1994; Karlsson et al., 2013; Kling et al.,
68 1991). However, these techniques were not tested for the simultaneous determination of several
69 dissolved gases, including CH₄ which is subject to rapid degassing during handling or storage if
70 samples are not preserved because of its low solubility in water (Duan & Mao, 2006). In addition,
71 some of the existing alternatives, such as filtration or field headspace equilibration, are difficult to
72 operate in remote areas in the field under harsh weather conditions and prone to potential ambient air
73 contamination. Solutions for water sample preservation should therefore involve a minimum of
74 manipulation steps in the field to avoid gas exchange with ambient air. Biocide amendments into

75 ~~sealed water bottles appears as one of the most efficient methods. Copper(II) chloride (CuCl₂) and~~
76 ~~silver nitrate (AgNO₃), the most toxic form of Silver, are relevant alternatives to HgCl₂ given their~~
77 ~~known toxicity (e.g., Ratte 2009; Amorim and Scott-Fordsmann 2012) and wide application in water~~
78 ~~treatments and water purification (Larrañaga et al., 2016; Nowack et al., 2011; NPIRS, 2023; Ullmann~~
79 ~~et al., 1985). Nevertheless, the efficiency of these alternative biocides has never been tested for~~
80 ~~dissolved gas samples preservation.~~

Formatted: Subscript

Formatted: Subscript

Formatted: Subscript

81 The addition of HgCl₂ to water is known to produce hydrochloric acid through hydrolysis (Ciavatta &
82 Grimaldi, 1968) and to form complexes with many environmental ligands, both inorganic (Powell *et*
83 *al.*, 2004) and organic (Tipping, 2007; Foti *et al.*, 2009; Liang *et al.*, 2019; Chen *et al.*, 2017). The
84 complexation of Hg⁺ with the carboxyl or thiol groups of ~~dissolved organic carbon~~DOC in oxic
85 environments could further increase the concentration of H⁺ (Khwaja et al., 2006; Skyllberg, 2008).

86 This acidification ~~could-can~~ be an issue in poorly buffered water (low ionic strength) with high
87 concentration of DOC where a shift in the pH and carbonate equilibrium ~~could-can~~ be induced. In that
88 case, the estimated CO₂ concentration would be higher after HgCl₂ fixation than the *in situ*

Formatted: Subscript

89 concentration, and if the shift in pH is not accounted for, can thus resulting in an overestimation of
90 dissolved CO₂ and bicarbonate concentrations. A similar acidification effect is also expected with

91 CuCl₂ amendments (Rippner et al., 2021), but not for AgNO₃ amendments. Such effects would not be
92 expected in marine water due to the high ionic strength of the water (Chou *et al.*, 2016) or freshwater
93 with low pH (<5.5) under which conditions nearly all dissolved inorganic carbon is CO₂ (Stumm &

Formatted: Subscript

Formatted: Subscript

94 Morgan, 1981). Thus, there are clear limits of the application of HgCl₂, and possibly CuCl₂, for
95 freshwater sample preservation given its risk of leading to overestimation of CO₂ and bicarbonate
96 concentrations, in addition to exposing field workers to the risks of its high toxicity.

Formatted: Subscript

Formatted: Subscript

97 ~~The use of HgCl₂ to preserve water samples prior to dissolved gas analyses is part of the current~~
98 ~~guidelines for greenhouse gas measurements in freshwater reservoirs (Machado Damazio et al., 2012;~~
99 ~~UNESCO/IHA, 2008, 2010). Hence, there is a risk of overestimating CO₂ concentrations and~~
100 ~~emissions, in absence of discrete measurement of emissions, from hydropower reservoirs with~~
101 ~~consequence on the present and expected greenhouse gas footprint from hydroelectricity. To ensure~~
102 ~~precise estimation of greenhouse gas emission from hydropower, the largest present and future~~
103 ~~renewable source of electricity (IEA, 2020), the use of HgCl₂ should therefore be discontinued.~~

104 Here we combine data from laboratory experiments (i) and field work (ii) to illustrate risks of mis-
105 estimation of dissolved gas concentrations in freshwaters with some preservatives and provide
106 recommendation for best practices in the field. First, we (i) performed some short-term and long-term
107 incubations of water from a typical heterotrophic unproductive boreal lake with circumneutral pH,
108 low ionic strength (poor buffering capacity) and high DOC concentration to tested the effect of
109 storage time and different preservative amendments of a natural water sample with circumneutral pH,

CO₂ overestimation from HgCl₂ fixation – Clayer et al.

110 ~~low ionic strength (poor buffering capacity) and high DOC concentration~~ on the determination of five
111 dissolved gases (O₂, CO₂, CH₄, N₂ and N₂O) by headspace equilibration and gas chromatography. ~~in~~
112 ~~The preservatives were the presence of~~ mercuric chloride (HgCl₂) ~~and~~ two alternative inhibitors,
113 chosen for their wide and effective application in water treatments and water purification (copper (II)
114 chloride – CuCl₂ and silver nitrate – AgNO₃; Xu & Imlay, 2012; Rai, Gaur & Kumar, 1981).
115 ~~Unamended water samples, where only ultrapure water was added, were also included for~~
116 ~~comparison, and a control (samples chilled in the dark at +4°C). In addition, we (ii) analysed~~
117 ~~dissolved CO₂ concentration data obtained from a typical productive boreal lake using two~~
118 ~~independent methods, one by gas chromatography following HgCl₂ fixation, and one through~~
119 ~~dissolved inorganic carbon determination without fixation. We further investigated the effect of~~
120 ~~preservation with HgCl₂ on the determination of dissolved CO₂ from water samples collected weekly~~
121 ~~during a full ice-free season from a lake experiencing varying pH conditions related to photosynthesis.~~
122 ~~Finally, w~~We show that the overestimation of dissolved CO₂ concentrations caused by HgCl₂ fixation
123 can be predicted based on chemical equilibria.

Formatted: Subscript

Formatted: Subscript

125 2. Methods

126 2.1. Effects of storage time and inhibitors on the ~~quantification~~determination of dissolved gases

127 ~~Study areasite and sampling~~

128 ~~Surface w~~Water samples ~~were~~as collected from Lake Svartkulp (59.9761313 N, 10.7363544 E;
129 Southeast Norway) north of Oslo, Norway, on the 4th of September 2019. ~~Lake water was carefully~~
130 ~~collected into A~~ 5 L plastic bottles ~~was gently pushed into the water and progressively tilted to let the~~
131 ~~water flow into the bottles without bubbling. The bottle aperture was covered with a 90 µm plankton~~
132 ~~net to~~ avoid sampling large particles. ~~This procedure was repeated five times to yield a total water~~
133 ~~volume of 25 L. The 5 L water bottles and~~were immediately brought back to the lab. Upon arrival at
134 the laboratory, ~~after temperature equilibration~~, water from the 5 L bottles ~~were~~was slowly poured, to
135 ~~avoid-limit~~ gas ~~exchange with the ambient airloss~~, into a 25 L tank to provide a single bulk sample to
136 start the incubation experiment. Filtration, e.g., with 0.45 or 0.2 µm filters, was avoided to minimize
137 changes in dissolved gas concentrations (e.g., Magen et al., 2014). The mixed water sample (25 L)
138 was sub-sampled (0.5 L) for the determination of alkalinity (127 µmol L⁻¹), pH (6.73), ammonium (3
139 µg N L⁻¹), nitrate (5 µg N L⁻¹), total N (230 µg N L⁻¹), phosphate (1 µg P L⁻¹), total P (9 µg P L⁻¹) ~~and~~
140 TOC (8.9 mg C L⁻¹) ~~and colour (59 mg L⁻¹ Pt)~~, all analysed by standard methods at the accredited
141 NIVA lab (see ~~Table-Tab.~~ S1). ~~In situ~~Temperature of the lake water was ~~measured with a handheld~~
142 ~~thermometer and was~~ 18.5 °C. ~~Note that particulate organic carbon is a negligible fraction of TOC in~~
143 ~~Norwegian lake waters, representing on average less than 3% (de Wit et al., 2023).~~

CO₂ overestimation from HgCl₂ fixation – Clayer et al.

Lake Svartkulp was selected for this experiment because it is representative of low ionic strength Northern Hemisphere lakes, typically found in granitic bedrock regions in North-East America and Scandinavia. It is a typical low-productivity, heterotrophic, slightly acidic to neutral, moderately humic lake. Similar lakes are found in Southern Norway (de Wit et al., 2023), large parts of Sweden (Valina et al. 2014), Finland, Atlantic Canada (Houle et al., 2022), Ontario, Québec, and North-East USA (Skjelkvåle and de Wit 2011; Weyhenmeyer et al., 2019).

Note that particulate organic carbon is a negligible fraction of TOC in Norwegian lake waters, representing less than 3% (de Wit et al., 2023).

Formatted: English (United States)

Laboratory incubation experiment with different preservatives and storage times

The experimental design involved to incubate 72 borosilicate glass bottles (120 mL) filled with lake water from our 25 L bulk sample and submitted to four different treatments: addition of 240µL of a preservative solution of (i) HgCl₂, (ii) CuCl₂, or a (iii) AgNO₃, or addition of 240 µL of (iv) MilliQ water. The bottles amended with MilliQ water are hereafter referred to as “unfixed”, and control, i.e., no added preservative). The 72 bottles were divide into three groups three time points of dissolved gas analysis (t=0, i.e., within 24h, which were incubated cold (+4°C) and dark for 24h, three weeks or three months respectively, before being processed for dissolved gas analysis by gas chromatography. These incubation times were selected to represent situations where samples are processed directly upon return to the laboratory (24h), or after medium (3 weeks) to long (3 months) -term storage, respectively, (t= 3 weeks and t= 3 months) and six replicates, yielding in total 72 experimental units. At each time point and for each treatment, a group of 6 bottles were further processed for dissolved gas analysis. Concentrations of O₂, N₂, N₂O, CO₂ and CH₄ were determined by gas chromatography (see below) using the headspace technique following Yang *et al.* (2015). Unfortunately, pH was not measured at the end of the storage period. The same day as the water samples were collected

In details, within 3h of lake water sampling, the 120mL bottles were gently filled with water from the mixed sample (25 L). Each 120mL bottle was slowly lowered into the water and progressively tilted to let the water flow into the bottle without bubbling. The bottle was then capped under water with a gas tight butyl rubber stopper after ensuring that there were no air bubbles in the bottle. was added gently to 72 borosilicate glass bottles (120 mL) and. The bottles were randomized prior to preservative or MilliQ amendment. The preservative solution or MilliQ amendment was pushed in each bottle with a syringe and needle through the rubber septum. To avoid overpressure, another needle was placed through septum at the same time, at least 2 cm above the other needle, to allow an equivalent volume of clean water to be released.

CO₂ overestimation from HgCl₂ fixation – Clayer et al.

178 Stock solutions of HgCl₂, CuCl₂ and AgNO₃ were prepared according to ~~Table-Tab. 1 using high~~
179 ~~accuracy chemical equipment (e.g., high accuracy scale, volumetric flasks). The Ag (Silver nitrate~~
180 ~~EMSURE® ACS; Merck KGaA, Germany) Cu (Copper(II) chloride dihydrate; Merck Life Science~~
181 ~~ApS, Norway) and Hg (Mercury(II) chloride; undetermined) salts were dissolved in MilliQ ultrapure~~
182 ~~water (>18 MΩ cm).~~ For measurement of CO₂ in seawater samples, the standard method involves
183 poisoning the samples by adding a saturated HgCl₂ solution in a volume equal to 0.05-0.02% of the
184 total volume (Dickson 2007). We used this as a starting point and added 0.02 % saturated HgCl₂
185 solution to ~~1/4th 18 bottles of the samples~~ (240 µL of HgCl₂ 10× diluted saturated solution), resulting
186 in a sample concentration of 14 µg HgCl₂ mL⁻¹ (51.6 µM; ~~Table-Tab. 1~~). Based on estimated toxicity
187 relative to Hg (Deheyn et al., 2004; Halmi et al., 2019), the silver and copper salts were added in
188 molar concentrations equal to two and three times the molar concentration of HgCl₂, respectively
189 (~~Table-Tab. 1~~), although it varies between species of microorganisms and environmental matrices
190 (Hassen et al., 1998; Rai, Gaur & Kumar, 1981). ~~CuCl₂ and AgNO₃, the most toxic form of Silver,~~
191 ~~were chosen because of their wide application in water treatments and water purification (Larrañaga~~
192 ~~et al., 2016; Nowack et al., 2011; NPIRS, 2023; Ullmann et al., 1985). Equal volume of MilliQ water~~
193 ~~was added to 1/4th of the samples as a control. The bottles were capped with gas tight butyl rubber~~
194 ~~stoppers after ensuring that there were no air bubbles in the samples. The samples for measurement of~~
195 ~~starting concentrations (t=0) were stored dark and cold (+4°C) overnight and analyzed within 24h of~~
196 ~~preparation, while the rest were stored dark and cold (+4°C) until measurement after 3 weeks (t=3w)~~
197 ~~and 3 months (t=3m) of storage. Concentrations of O₂, N₂, N₂O, CO₂ and CH₄ were determined by~~
198 ~~gas chromatography (see below) using the headspace technique following Yang et al. (2015).~~
199 ~~Unfortunately, pH was not measured at the end of the storage period.~~

Formatted: Font: (Default) Times New Roman

200 **Table 1.** Stock and sample concentrations of HgCl₂, CuCl₂ and AgNO₃.

Salt	Stock solution	Sample concentration	Rationale
HgCl ₂	70 g/L (saturated)	14.0 µg/mL (51.6 µM)	Dickson, Sabine & Christian, 2007
CuCl ₂	131.9 g/L	26.4 µg/mL (154.7 µM)	3 × Hg
AgNO ₃	87.6 g/L	17.5 µg/mL (103.1 µM)	2 × Hg

201
202 *Additional 24h incubation experiment with different preservatives for pH measurements*
203 Since pH was not measured at the end of the first incubation experiment, we performed an additional
204 experiment to document any potential rapid (within 24h) impacts of preservative on pH. A total of 48
205 borosilicate glass bottles (120 mL) filled with lake water were submitted to the same four different
206 treatments as the first experiment described above: HgCl₂, CuCl₂, AgNO₃ or MilliQ water
207 amendments. To this end, a 20L water tank was filled with surface water from Lake Svartkulp on the
208 14th of December 2023. The water tank was immediately returned to the laboratory and left for 24h to

Formatted: Subscript

Formatted: Subscript

Formatted: Subscript

Formatted: Superscript

CO₂ overestimation from HgCl₂ fixation – Clayer et al.

209 equilibrate to the room temperature. On December 15th, 120mL bottles were gently filled with water
210 from the bulk 20L sample, as described above. The bottles were randomized prior to preservative or
211 MilliQ amendment performed as described above. The bottles were then incubated at room
212 temperature for 2h or 24h. pH was measured in the initial unamended lake water, in 24 bottles opened
213 after 2h incubation, and in 24 bottles opened after 24h incubation. pH measurements were performed
214 with a WTW Multi 3620 pH meter calibrated using a two-point calibration at pH = 4 and pH = 7. All
215 pH measures were corrected for temperature. Water temperature of the water samples during pH
216 measurements ranged between 19.1 and 21.2°C.

Formatted: Superscript

Formatted: Font: Not Italic

218 2.2. Effects of HgCl₂ on dissolved CO₂ analyses over a range of pH values

219 *Lake Lundebyvannet time series* Study site and sampling

220 Water samples were collected from Lake Lundebyvannet located southeast of Oslo (59.54911 N,
221 11.47843 E, Southeast Norway). ~~The lake has a surface area of 0.4 km² and a maximum depth of~~
222 ~~5.5 m.~~ Two sets of S₂ samples were taken from 1, 1.5, 2 and 2.5 m depth using a water sampler once or
223 twice a week between April 2020 and January 2021 for the determination of (i) dissolved CO₂ by GC
224 analysis following fixation with HgCl₂ and (ii) DIC analysis with a TOC analyser. Samples for GC
225 analysis were filled into 120 mL glass bottles (as described above for the 72 incubation bottles),
226 which were sealed with rubber septa under water immediately without air bubbles. Samples for GC
227 analysis were ~~preservation-preserved prior to GC analysis (within 24h) was ensured by adding in the~~
228 field by adding a half-saturated (at 20°C) solution of HgCl₂ (150 µL) through the rubber seal of each
229 bottle using a syringe, as described above the 72 incubation bottles directly after sampling, resulting
230 in a concentration of 161 µM similar to previous studies (Clayer et al., 2021; Hessen et al., 2017;
231 Yang et al., 2015). Samples for DIC analysis were filled without bubbles in 100 ml Winkler glass
232 bottles that were sealed airtight directly after sampling. These samples were not fixed in any way and
233 were analysed by a TOC analyzer and a pH meter within two hours. Lake water (Temperature and pH
234 were measured in-situ using a HOBO pH data loggers placed at 1, 1.5, 2 and 2.5 m (Elit, Gjerdrum,
235 Norway).

Formatted: Subscript

Formatted: Subscript

236 The lake Lake Lundebyvannet has a surface area of 0.4 km² and a maximum depth of 5.5 m. It often
237 experiences large blooms of G. semen over the summer between May and September (Hagman et al.,
238 2015; Rohrlack, 2020). The lake water ~~was is~~ characterised by high and fluctuating concentrations of
239 humic substances (with DOC concentrations ranging from 8 to 28 mg C L⁻¹), ammonium (5 to 100 µg
240 N L⁻¹), nitrate (20 to 700 µg N L⁻¹), total N (average of 612 µg N L⁻¹), phosphate (2 to 4 µg P L⁻¹),
241 total P (average of 28 µg P L⁻¹; Rohrlack et al., 2020; Hagman et al., 2015), a fluctuating pH (from 5.5
242 to 7.3), weak ionic strength with alkalinity ranging between 30 and 150 µmol L⁻¹, and electric
243 conductivity varying from 40 to 70 µS cm⁻¹. ~~Temperature and pH were measured in situ using a~~

Formatted: Superscript

CO₂ overestimation from HgCl₂ fixation – Clayer et al.

244 ~~HOBO pH data logger placed at 1, 1.5, 2 and 2.5 m (Elit, Gjørdum, Norway)~~ For more details, see
245 Rohrlack *et al.* (2020).

246 Lake Lundebyvannet was selected for this experiment because it is representative of productive, low-
247 ionic strength Northern Hemisphere lakes typically found in the southern part of granitic bedrock
248 regions in North-East America and Scandinavia.

249 2.3. Analytical chemistry

250 *Gas chromatography*

251 Headspace was prepared by gently backfilling sample bottles with 20–30 mL helium (He; 99,9999%)
252 into the closed bottle while removing a corresponding volume of water. Care was taken to control the
253 headspace pressure within 5% of ambient and a slight He overpressure was released before
254 equilibration. The bottles were shaken horizontally at 150 rpm for 1 h to equilibrate gases between
255 sample and headspace. The temperature during shaking was recorded by a data logger. Immediately
256 after shaking, the bottles were placed in an autosampler (GC-Pal, CTC, Switzerland) coupled to a gas
257 chromatograph (GC) with He back-flushing (Model 7890A, Agilent, Santa Clara, CA, US).
258 Headspace gas was sampled (approx. 2 mL) by a hypodermic needle connected to a peristaltic pump
259 (Gilson Minipuls 3), which connected the autosampler with the 250 µL heated sampling loop of the
260 GC.

261 The GC was equipped with a 20-m wide-bore (0.53 mm) Poraplot Q column for separation of CH₄,
262 CO₂ and N₂O and a 60 m wide-bore Molsieve 5Å PLOT column for separation of O₂ and N₂, both
263 operated at 38°C and with He as carrier gas. N₂O and CH₄ were measured with an electron capture
264 detector run at 375°C with Ar/CH₄ (80/20) as makeup gas, and a flame ionization detector,
265 respectively. CO₂, O₂, and N₂ were measured with a thermal conductivity detector (TCD). Certified
266 standards of CO₂, N₂O, and CH₄ in He were used for calibration (AGA, Germany), whereas air was
267 used for calibrating O₂ and N₂. The analytical error for all gases was lower than 2%. For the Lake
268 Lundebyvannet time series, CO₂ was separated from other gases using the 20 m wide-bore (0.53 mm)
269 Poraplot Q column while the other gases were not measured.

270 The results from gas chromatography give the relative concentration of dissolved gases (in ppm) in
271 the headspace in equilibrium with the water. For the lab experiment with Svartkulp samples (section
272 2.1), the concentration of dissolved gases in the water at equilibrium with the headspace were
273 calculated from the solubility of gases in temperature corrected Henry constant in water using Carroll,
274 Slupsky and Mather (1991) for CO₂, Weiss and Price (1980) for N₂O, Yamamoto, Alcauskas and
275 Crozier (1976) for CH₄, Millero, Huang and Laferiere (2002) for O₂, Hamme and Emerson (2004) for
276 N₂. For the Lake Lundebyvannet time series (section 2.2), the concentration of CO₂ in the water
277 samples were determined using temperature-dependent Henry's law constants given by Wilhelm,

CO₂ overestimation from HgCl₂ fixation – Clayer et al.

278 Battino and Wilcock (1977). The quantities of gases in the headspace and water were summed to find
279 the concentrations and partial pressures of dissolved gases from the water collected in the field as
280 follows:

$$281 [gas] = \frac{p_{gas}HV_{water} + \frac{p_{gas}V_{headspace}}{RT}}{V_{water}} \quad \text{(Eq. 1)}$$

282 where [gas] is the gas aqueous concentration, p_{gas} is the gas partial pressure, H is the Henry constant,
283 V_{water} is the volume of water sample during headspace equilibration, $V_{headspace}$ is the headspace gas
284 volume during equilibration, R is the gas constant and T the temperature during headspace
285 equilibration (recorded during shaking). The calculations were similar to Yang *et al.* (2015).

286

287 *DIC analyses*

288 DIC analysis was performed for the Lake Lundebyvannet time series using a Shimadzu TOC-V CPN
289 (Oslo, Norway) instrument equipped with a non-dispersive infrared (NDIR) detector with O₂ as a
290 carrier gas at a flow rate of 100 mL min⁻¹. Two to three replicate measurements were run per sample.
291 The system was calibrated using a freshly prepared solution containing different concentrations of
292 NaHCO₃ and Na₂CO₃. CO₂ concentrations in water samples ($[CO_2]$) were calculated on the bases of
293 temperature, pH and DIC concentrations as follows (Rohrlack *et al.*, 2020):

$$294 [CO_2] = \frac{[H^+]^2 C_T}{Z} \quad \text{(Eq. 2)}$$

295 where $[H^+]$ is the proton concentration (10^{-pH}), C_T is the dissolved inorganic carbon concentration
296 and Z is given by:

$$297 Z = [H^+]^2 + K_1[H^+] + K_1K_2 \quad \text{(Eq. 3)}$$

298 where K_1 and K_2 are the first and second carbonic acid dissociation constant adjusted for temperature
299 ($pK_1 = 6.41$ and $pK_2 = 10.33$ at 25°C; Stumm & Morgan, 1996).

300

301 2.4. Data analysis

302 *pCO₂ and saturation deficit*

303 Lake Lundebyvannet CO₂ concentrations provided by GC and DIC analyses were converted to pCO₂
304 (in μatm) as follows:

$$305 pCO_2 = \frac{[CO_2]}{0.987 \times K_H P_{atm}} \quad \text{(Eq. 4)}$$

CO₂ overestimation from HgCl₂ fixation – Clayer et al.

306 where K_H is Henry constant for CO₂ adjusted for in-situ water temperature (Stumm & Morgan, 1996)
307 and P_{atm} is the atmospheric pressure in bar given by:

$$P_{atm} = (1013 - 0.1 \times altitude) \times 0.001 \quad (\text{Eq. 45})$$

309 where *altitude* is the altitude above sea level of Lake Lundebyvannet (158 m). Finally, the CO₂
310 saturation deficit (Sat_{CO_2} in μatm) was approximated given by

$$Sat_{CO_2} = pCO_2 - [CO_2]_{air} \quad (\text{Eq. 56})$$

312 where $[CO_2]_{air}$ is the pCO₂ in the air (416 μatm for 2020 in Southern Norway retrieved from EBAS
313 database; NILU, 2022; Tørseth et al., 2012). Sat_{CO_2} gives the direction of CO₂ flux at the air-water-
314 atmosphere interface, and its product with gas transfer velocity determine the CO₂ flux at the water-
315 atmosphere interface, i.e., whether lake ecosystems are sink ($Sat_{CO_2} < 0$) or source ($Sat_{CO_2} > 0$) of
316 atmospheric CO₂.

317

318 *Statistical analyses*

319 The effect of storage time and treatment on five dissolved gases (O₂, N₂, CO₂, CH₄, N₂O) from the
320 Lake Svartkulp samples was tested with a two-way ANOVA at an alpha level adapted using the
321 Bonferroni correction for multiple testing, i.e., $\alpha=0.05/5=0.01$. To evaluate the impact of Hg fixation
322 on Lake Lundebyvannet samples, $[CO_2]$ values determined by headspace equilibration and GC
323 analysis of HgCl₂-fixed samples were compared with those calculated from DIC measurements of
324 unfixed samples with a paired t-test.

325 A regression analysis was performed to describe the overestimation of CO₂ concentrations caused by
326 HgCl₂ fixation in Lake Lundebyvannet samples as a function of pH. The total CO₂ concentration in
327 the HgCl₂-fixed samples ($[CO_2]_{HgCl_2}$) can be expressed as:

$$[CO_2]_{HgCl_2} = [CO_2]_i + [CO_2]_{ex} \quad (\text{Eq. 67})$$

329 where $[CO_2]_i$ is the initial CO₂ concentration prior to HgCl₂ fixation, i.e., CO₂ concentration in the
330 unfixed samples, and $[CO_2]_{ex}$ is the excess CO₂ concentration caused by a decrease in pH following
331 HgCl₂ fixation. The relative CO₂ overestimation (E in %) is given by:

$$E = \frac{[CO_2]_{HgCl_2} - [CO_2]_i}{[CO_2]_i} = \frac{[CO_2]_{ex}}{[CO_2]_i} \quad (\text{Eq. 78})$$

333 The impact of pH (or $[H^+]$) on E was mathematically described by running a regression analysis
334 using MATLAB®. The *fminsearch* MATLAB function from the Optimization toolbox was used to
335 find the minimum sum of squared residuals (SSR) for functions of the form of: $E = A/[H^+]$ or $E =$

CO₂ overestimation from HgCl₂ fixation – Clayer et al.

336 $A \times 10^{-B \times pH}$. For each optimal solution, the root-mean-square error (RMSE) and coefficient of
337 determination (R^2) were calculated against observed values of E , i.e., values of E determined
338 empirically from observed $[CO_2]_i$ and $[CO_2]_{ex}$.

339

340 *Chemical speciation, saturation-index calculations, and prediction of CO₂ overestimation*

341 The speciation of solutes and saturation index values (SI) of selected minerals were calculated with
342 the program PHREEQC developed by the USGS (Parkhurst & Appelo, 2013), neglecting the effect of
343 dissolved organic matter. This was used to assess the impact of the addition of preservative on shifting
344 the carbonate equilibrium as well as dissolved inorganic carbon losses due to carbonate mineral
345 precipitation. For each PHREEQC simulation, two files, respectively the database (with input
346 reactions) and input files, were used to define the thermodynamic model and the type of calculations
347 to perform. The database of MINTEQA2 (e.g., *minteq.dat*, Allison et al., 1991) was used to describe
348 the chemical system because it includes, inter alia, reactions and constants for Ag, Cu and Hg
349 complexation with Cl, NO₃ and carbonates. In total, three simulations were run representing the
350 addition of each preservative solution to sample water from Lake Svartkulp. The input files described
351 the composition of two aqueous solutions: (i) the preservative solution assumed to contain only the
352 preservative and (ii) sample water from Lake Svartkulp with observed major element concentrations
353 (pH, Al, Ca, Cl, Cu, Fe, Mg, Mn, N as nitrate, K, Na, S as sulfate, Zn; Table-Tab. S1) and Hg and Ag
354 concentration assumed to be 10⁻⁵ mg/L. The output file provided the activities of the various solutes in
355 the preserved samples, i.e., simulating the mixing of 120 mL of lake water with 240 μL of the AgNO₃,
356 CuCl₂ and HgCl₂ preservative solutions, as described in section 2.1. This procedure allows to estimate
357 the pH of the preserved samples as well as SI for various mineral phases. The SI is calculated by
358 PHREEQC comparing the chemical activities of the dissolved ions of a mineral (ion activity product,
359 IAP) with their solubility product (K_s). When SI > 1, precipitation is thermodynamically favourable.
360 However, PHREEQC does not give information about precipitation kinetics.

361 PHREEQC was also used to estimate the decrease in pH caused by adding 150 μL of a half-saturated
362 HgCl₂ solution to Lake Lundebyvannet samples prior to GC analyses, as described in section 2.2. In
363 absence of data on the chemical composition of Lake Lundebyvannet, we assumed that it had the
364 same composition as Lake Svartkulp water samples. This assumption is supported by the fact that
365 waters from both lakes have circumneutral pH, low ionic strength (poor buffering capacity) and high
366 DOC concentration and would therefore behave similarly in presence of acids. Briefly, for each 0.1
367 pH value between pH of 5.4 and 7.3, the carbonate alkalinity was first adjusted by increasing HCO₃
368 concentrations in the input files for PHREEQC to confirm that the water was at equilibrium at the
369 given pH value. Then, the effect of adding 150 μL of a half-saturated HgCl₂ solution was simulated as
370 described above for Lake Svartkulp. Knowing the new equilibrated pH, after addition of HgCl₂, the

CO₂ overestimation from HgCl₂ fixation – Clayer et al.

371 overestimation of CO₂ concentration in Hg-fixed samples relative to unfixed samples (*E*, described in
372 Eq. 7-8 above) can be predicted as described below.

373 Adapting Eq. (42), we obtain:

$$374 \quad [CO_2]_{HgCl_2} = \frac{[H^+]_{HgCl_2}^2 C_T}{Z_{HgCl_2}} \quad (\text{Eq. 89})$$

375 and

$$376 \quad [CO_2]_i = \frac{[H^+]_i^2 C_T}{Z_i} \quad (\text{Eq. 910})$$

377 where $[H^+]_i$ is the proton concentration measured in the initial water samples prior to HgCl₂ fixation,
378 and $[H^+]_{HgCl_2}$ is the proton concentration estimated by PHREEQC following HgCl₂ fixation, and
379 similarly for Z_i and Z_{HgCl_2} from Eq. (23). Combining Eqs. (67), (89) and (910) we obtain:

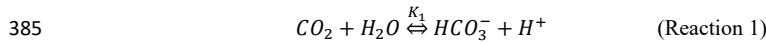
$$380 \quad [CO_2]_{ex} = C_T \left(\frac{[H^+]_{HgCl_2}^2}{Z_{HgCl_2}} - \frac{[H^+]_i^2}{Z_i} \right) \quad (\text{Eq. 1011})$$

381 Hence:

$$382 \quad E = \frac{[CO_2]_{ex}}{[CO_2]_i} = \frac{\left(\frac{[H^+]_{HgCl_2}^2}{Z_{HgCl_2}} - \frac{[H^+]_i^2}{Z_i} \right)}{\frac{[H^+]_i^2}{Z_i}} \quad (\text{Eq. 1112})$$

383

384 Alternatively, *E* can also simply be predicted based on the carbonic acid dissociation:



386 At equilibrium, we have:

$$387 \quad K_1 = \frac{[HCO_3^-][H^+]}{[CO_2]} \quad (\text{Eq. 1213})$$

388 When pH is decreased upon addition of HgCl₂, a fraction (α) of the initial bicarbonate concentration
389 $[HCO_3^-]_i$ is turned into CO₂. This fraction, expressed as $[CO_2]_{ex}$ in Eq. (67) above, can be estimated
390 with Eq. 12-13 as follows:

$$391 \quad [CO_2]_{ex} = \alpha [HCO_3^-]_i = \frac{\alpha K_1 [CO_2]_i}{[H^+]_i} \quad (\text{Eq. 1314})$$

392 Introducing the expression of $[CO_2]_{ex}$ from Eq. 13-14 into Eq. 7-8 yields:

$$393 \quad \frac{[CO_2]_{ex}}{[CO_2]_i} = E = \frac{\alpha K_1}{[H^+]_i} \quad (\text{Eq. 1415})$$

394 When the decrease in pH, or acidification, is greater than the buffering capacity of the water: $\alpha = 1$.
 395 The value of α cannot exceed 1 because the amount of CO₂ produced by a decrease in pH cannot
 396 exceed the amount of HCO₃⁻ initially present. In all the other cases, we have: $\alpha < 1$. For both
 397 predictions of E , i.e., with Eqs. 4412 and 4415, the root-mean-square error (RMSE) and coefficient
 398 of determination (R²) were calculated.

399 Finally, additional sources of CO₂ overestimation were investigated by analysing the residuals of the
 400 model described by Eq. 4412, i.e., the difference between E predicted with Eq. 4412 and E
 401 determined empirically with Eq. 78. Briefly, residuals were plotted against pH and *in situ*
 402 temperature. Residuals were separated in two groups based on the empirical value of [HCO₃⁻]_{*i*} –
 403 [CO₂]_{*ex*}, i.e., the first group had values of [HCO₃⁻]_{*i*} – [CO₂]_{*ex*} ≥ a while the second group had
 404 values of [HCO₃⁻]_{*i*} – [CO₂]_{*ex*} ≤ $-a$ where different values for a were used: 20, 10 or 5 μM. The
 405 justification for separating residuals in two groups is that: (i) the first group represents samples for
 406 which bicarbonate alkalinity in the original sample is, as expected, higher than CO₂ overestimation
 407 after HgCl₂-fixation, while (ii) the second group represents samples for which bicarbonate alkalinity
 408 is not sufficient to explain CO₂ overestimation after HgCl₂-fixation.

409

410 CO₂ diffusion fluxes from Lake Lundebyvannet

411 The diffusive flux of CO₂ (F_{CO_2} in mol m⁻² d⁻¹) from Lake Lundebyvannet surface water was
 412 estimated according to:

$$413 \quad F_{CO_2} = \frac{k_{CO_2}([CO_2] - [CO_2]_{eq})}{1000} \quad (\text{Eq. 4416})$$

414 where k_{CO_2} is the CO₂ transfer velocity in m d⁻¹, [CO₂] is the surface water CO₂ concentration (μM),
 415 and 1000 is a factor to ensure consistency in the units and [CO₂]_{*eq*} is the theoretical water CO₂
 416 concentration (μM) in equilibrium with atmospheric CO₂ concentration calculated with Eq. (3) and
 417 pCO₂ of 416 μatm (see above).

418 The CO₂ transfer velocity (k_{CO_2}) was estimated as follows (Vachon & Prairie, 2013):

$$419 \quad k_{CO_2} = k_{600} \left(\frac{600}{Sc_{CO_2}} \right)^{-n} \quad (\text{Eq. 4417})$$

420 where k_{600} is the gas transfer velocity (m d⁻¹) estimated from empirical wind-based models and Sc_{CO_2}
 421 is the CO₂ Schmidt number for in situ water a given temperature (unitless; Wanninkhof, 2014). We
 422 used n values of 0.5 or 2/3 when wind speed was below or above 3.7 m s⁻¹, respectively (Guérin et al.,
 423 2007). Empirical k_{600} models included those from Cole & Caraco (1998; $k_{600} = 2.07 + 0.215U_{10}^{1.7}$),
 424 Vachon & Prairie (2013; $k_{600} = 2.51 + 1.48U_{10} + 0.39U_{10} \log_{10} LA$) and Crusius & Wanninkhof

CO₂ overestimation from HgCl₂ fixation – Clayer et al.

425 (2003; power model: $k_{600} = 0.228U_{10}^{2.2} + 0.168$ in cm h^{-1}). U_{10} and LA refer to mean wind speed at
426 10 m in m s^{-1} and lake area in km^2 , respectively. Sub-hourly U_{10} data for 2020 was retrieved from a
427 weather station of the Norwegian Meteorological Institute located 1.5 km west of Lake
428 Lundebyvannet (station name: E18 Melleby; ID: SN 3480; 59.546 N, 11.4535E) using the Frost
429 application programming interface (*Frost API*, 2022). Daily, monthly, and yearly (only covering the
430 ice-free season: April–November) F_{CO_2} was estimated using Eq. (12). Daily $[\text{CO}_2]$ was interpolated
431 from weekly data using a modified Akima spline (makima spline in Matlab® based on Akima, 1974).
432 This interpolation method is known to avoid excessive local undulations.

433 3. Results and discussion

434 3.1. Effects of inhibitors-preserved and storage time on dissolved gases

435 In the ~~control-unfixed~~ samples from Lake Svartkulp, the concentration of O₂ declined while CO₂
436 increased over time in a close to 1:1 molar ratio, likely reflecting the effect of microbial respiration
437 activity and mineralisation of organic matter (Fig. 1, ~~Table Tab. S2~~). Concentration of O₂ in the
438 ~~control-unfixed~~ decreased from near 300 to below 200 μM (Fig. 1). In the presence of inhibitors, O₂
439 concentrations tended to be slightly higher at $t=0-24\text{h}$ and remained constant or declined only slightly
440 over time to generally remain at or above saturation (280 to 300 μM). Thus, the inhibitors were
441 effective in reducing oxic respiration.

442 The concentration of CO₂ in the presence of AgNO₃ at $t = 0-24\text{h}$ was not significantly different to the
443 ~~control-unfixed~~ at $t = 0$ (Fig 1; paired t-test, $P>0.1$). At $t = 0-24\text{h}$, CO₂ concentrations were however
444 much higher in the presence of HgCl₂ (135 μM) or CuCl₂ (131 μM) than in the ~~control-unfixed~~ (89
445 μM ; Fig 1, ~~Table Tab. S2~~). ~~This is likely due to an acidification of the poorly buffered (alkalinity 127~~
446 ~~μM) and near neutral water (pH=6.73), shifting the carbonate equilibrium from HCO₃⁻ to CO₂ as also~~
447 ~~shown by Borges et al. (2019).~~ ~~The increase of CO₂ further increases from 130 μM to ~160 μM after~~
448 ~~3 weeks in both sample sets preserved with HgCl₂ and CuCl₂ while a decrease in O₂ is less~~
449 ~~pronounced not mirrored by a similar decrease in O₂ for samples fixed with CuCl₂ and completely~~
450 ~~absent for samples fixed with HgCl₂. This suggests that oxic respiration is not the main source for this~~
451 ~~additional 30 μM of CO₂ but rather points towards additional acidification of the samples caused by~~
452 ~~kinetically controlled complexation of Hg²⁺ with dissolved organic matter (Miller et al., 2009). In fact,~~
453 ~~the relatively slow complexation of Hg²⁺ with organic thiol groups can release two protons~~
454 ~~(Skylberg, 2008) and up to three, with some participation of a third weak acid group (Khawaja et al.,~~
455 ~~2006). The following decrease in CO₂ after 3 months (down to ~145 μM) points to other processes.~~
456 Overall, the addition of HgCl₂ or CuCl₂ following sampling increased CO₂ concentrations by 47%
457 ~~within the first after 24h compared to the control-unfixed~~ and caused further changes over the three-
458 month storage time, while preservation with AgNO₃ yielded CO₂ concentrations consistent with the
459 ~~control-unfixed~~ and caused negligible changes over time (Fig. 1; paired t-test, $P>0.1$).

Formatted: Subscript

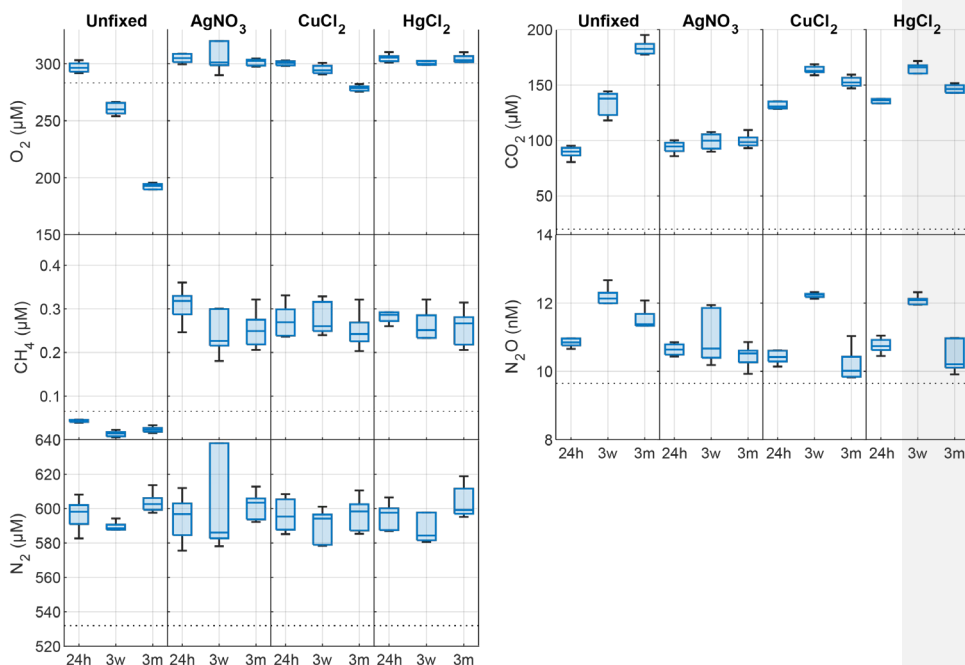
Formatted: Subscript

Formatted: Not Superscript/ Subscript

Formatted: Subscript

CO₂ overestimation from HgCl₂ fixation – Clayer et al.

460 The concentration of CH₄ across all samples ranged between 0.017 and 0.377 μM (Fig. 1), as
461 expected two orders of magnitude smaller than CO₂. At t = ~~0~~24h, the concentration of CH₄ was over
462 0.2 μM in the presence of inhibitors while it was below saturation in the ~~control-unfixed~~ (0.03 μM;
463 Fig. 1). CH₄ oversaturation in the preserved samples persisted after three weeks and three months of
464 storage and CH₄ concentration remained constant unchanged (Fig. 1, Table-Tab. S2). ~~Both~~
465 ~~observations are consistent with the fact that the three preservatives were effective in preserving CH₄~~
466 ~~from oxidation. Even at t = 0, i.e., for samples analysed within 24h after sampling, preservatives are~~
467 ~~required to preserve CH₄ in oxic samples.~~



468

469 **Fig 1.** Changes in dissolved O₂, CO₂, CH₄, N₂O and N₂ concentrations (nM or µM) in the absence
 470 (~~control~~unfixed) and presence of different preservatives (AgNO₃, CuCl₂, HgCl₂) at three times (~~0~~24h,
 471 ~~day after sample collection~~24h after incubation start; 3w, three weeks after collection; 3m, three
 472 months after collection). The horizontal dotted line is the saturated gas concentration corresponding to
 473 100% gas saturation at *in situ* lake temperature. Box plots show the median, 25th and 75th percentiles
 474 and the whiskers display all data coverage.

Formatted: Superscript

Formatted: Superscript

CO₂ overestimation from HgCl₂ fixation – Clayer et al.

475 ~~In fact, oxic methanotrophy typically show rates in the order of $\mu\text{M day}^{-1}$ (Thottathil et al., 2019; van~~
476 ~~Grinsven et al., 2021). Hence, a CH₄ consumption of 0.3 μM within 24h in the unpreserved, control~~
477 ~~water samples is realistic (Fig. 1).~~

478 The concentration of N₂O ranged between 9.8 and 12.7 nM with only samples preserved with AgNO₃
479 showing negligible changes over time (Fig. 1; paired t-test, P>0.1). All the other samples showed
480 consistent patterns with storage time. N₂O concentrations initially increased within the first 3 weeks,
481 followed by a decrease after 3 months. ~~Similar patterns of net N₂O production followed by net~~
482 ~~consumption were also reported in short term incubations of seawater from the high latitude Atlantic~~
483 ~~Ocean, although over much shorter timescales, i.e., 48 and 96h (Rees et al., 2021). The lack of~~
484 ~~inhibition of N₂O production and consumption in the samples preserved with HgCl₂ and CuCl₂ can be~~
485 ~~attributed to the fact that N₂O production tends to increase under increasing acidic conditions~~
486 ~~(Knowles, 1982; Morkved et al., 2007; Seitzinger, 1988). In fact, the mole fraction of N₂O produced~~
487 ~~during denitrification increases compared to N₂ as pH decreases (Knowles, 1982). In summary,~~
488 ~~AgNO₃ appears to be the only preservative inhibiting N₂O cycling, although further tests with a larger~~
489 ~~range of N₂O concentrations are required to confirm its efficiency.~~

490 The changes in N₂ were likely within handling and analytical errors and not different in the presence
491 or absence of inhibitors (Fig. 1; ~~Table Tab. S2; paired t-test, P>0.1~~).

493 3.2. Effects of preservatives on pH

494 ~~In the samples amended with ultrapure water or AgNO₃, the pH did not show any significant changes~~
495 ~~after 2h or 24h. In contrast, both groups with HgCl₂ and CuCl₂ amendments show significant~~
496 ~~decreases of pH after 2h, -0.12 and -0.19, respectively, and 24h, -0.16 and -0.21, respectively. In~~
497 ~~addition, they showed a significant decrease in pH from 2h to 24h. Samples amended with CuCl₂~~
498 ~~show that strongest decrease in pH.~~

Formatted: Subscript

Formatted: Subscript

Formatted: Subscript

Formatted: Subscript

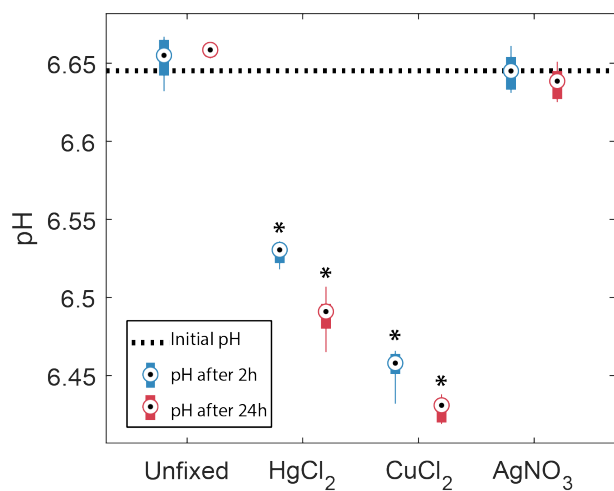


Fig 2. Changes in pH in the absence (unfixed) and presence of different preservatives (AgNO₃, CuCl₂, HgCl₂) at two times, 2h and 24h after the start of the incubation. The horizontal dotted line represents the initial pH of the bulk water sample. Box plots show the median, 25th and 75th percentiles and the whiskers display all data coverage of the 6 replicates. Stars indicate groups that are significantly different from each other and from the initial pH (two-way ANOVA).

3.23. Contrasting impacts of HgCl₂, CuCl₂ and AgNO₃ on dissolved CO₂ estimation revealed by chemical speciation modelling

The PHREEQC simulation of unpreserved samples, based on concentrations of all major elements (Table Tab. S1), predicted a pH of 6.72 (Table Tab. 2) which is very close to the measured pH of 6.73 (Table Tab. S1). This suggests that chemical information provided to PHREEQC is likely sufficient to describe the system, without having to invoke more complex reactions with dissolved organic matter.

The addition of HgCl₂ and CuCl₂ both caused a significant decrease in pH to 6.40 and 6.45, respectively (Table Tab. 2). The proximity of these pH values to the first carbonic acid dissociation constant (pK_{a1} = 6.41 at 25°C; Stumm & Morgan, 1996) implies a significant shift in the carbonate equilibrium from HCO₃⁻ to CO₂. In fact, introducing pH and CO₂ concentration values of 6.41–6.45 and 130 μM, respectively, for the samples preserved with HgCl₂ and CuCl₂ into Eqs. 1 and 2 yields DIC concentrations (C_{DIC}) of about 270 μM at t=0. These DIC concentrations are almost equal to those calculated for the control and samples preserved with AgNO₃ at t=0, i.e., with a pH of 6.73 and CO₂ concentration of 88 μM. Interestingly, the concentration of CO₂ in the samples preserved with HgCl₂ and CuCl₂ continue to increase up to ~160 μM after 3 weeks. Given that oxic respiration is inhibited (Fig. 1), this additional CO₂ is believed to originate from progressive release of protons following relatively slow complexation of Hg²⁺ with dissolved organic matter (Khawaja et al., 2006; Miller et al.,

CO₂ overestimation from HgCl₂ fixation – Clayer et al.

~~2009; Skjellberg, 2008). Note that PHREEQC could not predict complexation of Hg²⁺ with dissolved organic matter given that we neglected the effect of dissolved organic matter.~~

In absence of preservatives, none of the common carbonate minerals, including calcite, were associated with a saturation index higher than 1, i.e., dissolution was thermodynamically favourable for all these minerals and no DIC loss was expected (Table-Tab. 2). However, upon addition of HgCl₂ or CuCl₂, some carbonate minerals, e.g., HgCO₃ or malachite and azurite, respectively, were expected to spontaneously precipitate given their relatively high saturation index values. ~~This observation can explain the consistent decrease in CO₂ concentrations observed between three weeks and three months for sampled treated with HgCl₂ and CuCl₂. Calcite precipitation is typically observed in supersaturated solutions within 48h (Kim et al., 2020). Hence, it is realistic to consider that Hg and Cu carbonate precipitation influenced the CO₂ concentration within the preserved samples over the three months of storage time. Impacts of Hg or Cu carbonate precipitation is not evident after three weeks likely because of slow but persistent CO₂ production in presence of HgCl₂ and CuCl₂ related to acidification as described above (Fig. 1). However, after three weeks, this production likely weakens and is counterbalanced by increasing carbonate precipitation.~~

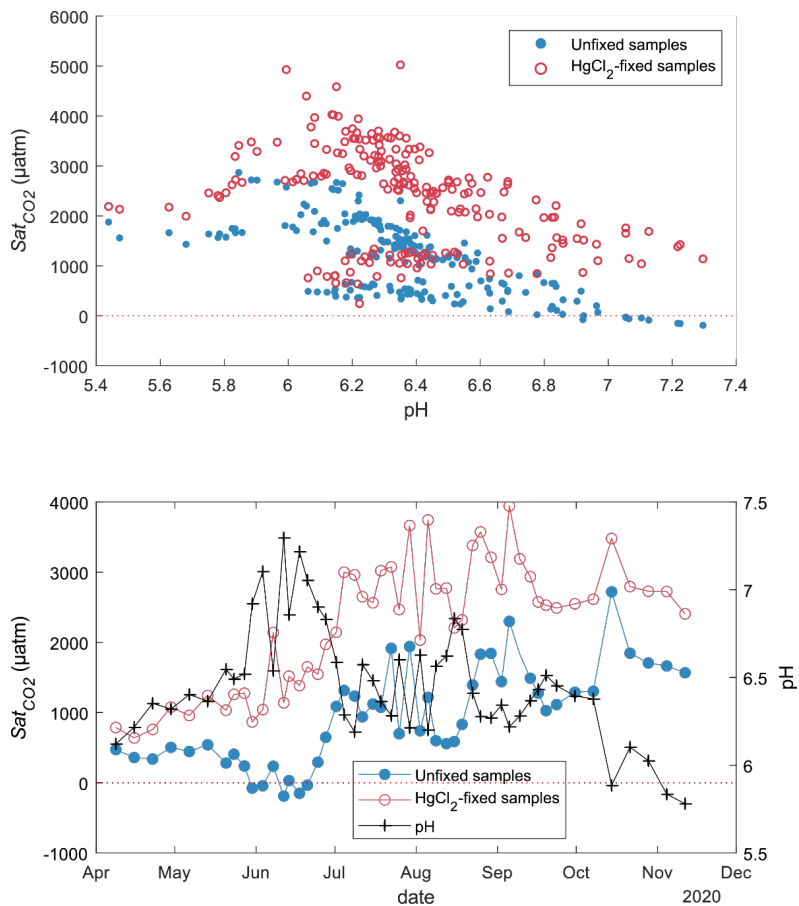
Table 2. pH and saturation indices of selected carbonate minerals estimated by PHREEQC for the unpreserved and preserved samples

Preservatives	pH	Saturation indices			
		HgCO ₃	Cu ₂ (OH) ₂ CO ₃ - Malachite	Cu ₂ (OH) ₂ CO ₃ - Azurite	Ag ₂ CO ₃
Unpreserved Unfixed	6.72	-2.31	-4.96	-8.71	-16.42
HgCl ₂	6.40	3.64	-5.89	-10.10	-17.20
CuCl ₂	6.45	-2.55	2.26	2.11	-17.44
AgNO ₃	6.71	-2.31	-4.97	-8.73	-4.33

3.3. Effects of HgCl₂ on dissolved CO₂ concentration under a range of pH

CO₂ concentrations in unfixed water samples from Lake Lundebyvannet were significantly lower than in the HgCl₂-fixed samples (mean difference: 52 μM; paired t-test; P<0.0001; Table-Tab. 3). Fixation with HgCl₂ caused a general overestimation of CO₂ concentration and the saturation deficit (Fig. 23), thus missing out events of CO₂ influx (carbon sink) under high photosynthesis activity (high pH; Fig. 23). ~~As for the samples from Lake Svartkulp described above, the overestimation in CO₂ concentration likely stems from the acidification by HgCl₂ (161 μM added) shifting the carbonate equilibrium towards CO₂.~~ In ~~parallel~~fact, PHREEQC predicted a decrease of 0.6 to 1.8 units of pH related to HgCl₂ addition (Fig. S1).

CO₂ overestimation from HgCl₂ fixation – Clayer et al.



550
551 **Figure 23.** CO₂ saturation deficit in Lake Lundebyvannet as a function of in situ pH for all unfixed
552 (obtained from DIC analysis) and HgCl₂-fixed (obtained from GC analysis) samples (top panel).
553 Timeseries of pH and CO₂ saturation deficit of Lake Lundebyvannet surface water (1-m deep) for
554 unfixed and HgCl₂-fixed samples (bottom panel).

CO₂ overestimation from HgCl₂ fixation – Clayer et al.

555 **Table 3.** CO₂ concentrations ([CO₂], μM) and diffusion fluxes (F_{CO₂}, mol m⁻² d⁻¹) from Lake
 556 Lundebyvannet estimated from HgCl₂-fixed and unfixed samples following Cole and Caraco (1998).
 557 Ice-free season spans April to November. Data are also shown in Fig. 5

Preservatives	Apr.	May	Jun.	Jul.	Aug.	Sep.	Oct.	Nov.	Ice-free season
[CO ₂]	HgCl ₂ No	45.3	39.0	18.719	687.9	59.2	85.4	123.4	119120.8
	ne	67.968	75.4	74.0	1332.9	129.913	149.4	179.3	178.4
	Diff (%)	+50.0%	+93.0%	+296.0%	+96.0%	+119.0%	+75.0%	+45.0%	+49.0%
F _{CO₂}	HgCl ₂ No	0.10	0.07	0.01	0.15	0.11	0.23	0.37	0.48
	ne	0.20	0.21	0.16	0.34	0.29	0.47	0.57	0.77
	Diff (%)	+97.0%	+188.0%	+2163.0%	+130.0%	+162.0%	+99.0%	+55.0%	+62.0%

558

559 The pH value of water samples from Lake Lundebyvannet varied between 5.4 and 7.3 (Fig 23 and
 560 34), mainly due to marked variations in phytoplankton photosynthetic activity (Rohrlack et al., 2020).
 561 The relative overestimation of CO₂ (*E*) follows an exponential increase with pH and is well
 562 reproduced by a simple exponential function ($2.56 \times 10^{-5} \times 10^{1.015 \times pH}$, RMSE=44%, R²=0.81,
 563 $p < 0.0001$; Fig. 34). ~~This exponential increase likely reflects the corresponding decrease in absolute
 564 CO₂ concentration with pH (Stumm & Morgan, 1981) concomitant here to phytoplankton
 565 photosynthesis (Fig. 2). In fact, the exponential increase in CO₂ overestimation is easily predicted by
 566 Eq. (8) with an equivalent level of accuracy than the optimized exponential function (Fig. 3).
 567 Consistently, the relative overestimation of CO₂ (*E*) shows an inverse decrease with [H⁺] that is well
 568 reproduced by a simple inverse function ($3.25 \times 10^{-5} / [H^+]$; RMSE=44%, R²=0.81, $p < 0.0001$; Fig.
 569 3) and predicted by Eq. (14), with an α value of 1. Combining Eqs. 7 and 14 and solving it with pH
 570 values estimated from PHREEQC (Fig. S1) for α yields values ranging between 0.72 and 0.89 with an
 571 average of 0.85. Unexpectedly, this average α value is almost equal to the ratio of the inverse function
 572 coefficient and K_{a1} , i.e., $\frac{3.25 \times 10^{-5}}{K_{a1}} = 0.87$. Hence, the relative overestimation of CO₂ (*E*) caused by
 573 HgCl₂ fixation is easily predicted by the change in bicarbonate equilibrium knowing the proton
 574 release from HgCl₂ addition.~~

575 In waters with higher ionic strength, the release of proton from HgCl₂ addition will likely be smaller.
 576 PHREEQC can be used to predict it, if sufficient knowledge is gathered on the ionic water
 577 composition. Proton release during HgCl₂ fixation can be represented by the following reaction:



Formatted: Font: 10 pt
 Formatted: Font: 10 pt
 Formatted: Font: 10 pt
 Formatted: Font: 10 pt
 Formatted: Subscript
 Formatted: Font: 10 pt
 Formatted: Font: 10 pt
 Formatted: Font: 10 pt
 Formatted: Font: 10 pt
 Formatted: Font: 10 pt
 Formatted: Font: 10 pt
 Formatted: Font: 10 pt
 Formatted: Font: 10 pt
 Formatted: Font: 10 pt
 Formatted: Font: 10 pt
 Formatted: Font: 10 pt
 Formatted: Font: 10 pt
 Formatted: Font: 10 pt
 Formatted: Font: 10 pt

579 ~~From reaction 2, it becomes evident that the initial concentration of chloride in the water samples will~~
580 ~~likely limit HgCl₂ dissociation and proton release. This is a likely mechanism occurring in seawater~~
581 ~~where HgCl₂ has been shown to cause a decrease in pH, although at a negligible level (Chou et al.,~~
582 ~~2016).~~

583 4. Discussion

584 Prior to using dissolved gas concentrations in freshwater to estimate the magnitude of biological
585 aquatic processes such as photosynthesis and oxic respiration, denitrification and methanogenesis, we
586 must ensure that biological activity between sampling and laboratory analyses was efficiently
587 inhibited without significant impacts on the sample's chemistry. Here we report a unique dataset on
588 the impact of three preservatives on water samples from a typical low-ionic strength, unproductive
589 boreal lake to inform on potential risks of mis-estimation of dissolved gas concentrations. We further
590 show, using CO₂ concentration data from a typical productive boreal lake, that using HgCl₂ can lead
591 to negligence of the role of photosynthesis in lake C cycling.

592 4.1 Best preservative for the determination of dissolved gas concentrations

593 Given that none of the four treatments (unfixed, HgCl₂, CuCl₂ or AgNO₃) applied to Lake Svartkulp
594 water samples during the 3-month incubation offer an independent control, a first challenge is to
595 determine which of the treatment represent the most realistic dissolved gas concentrations close to
596 real condition. For CO₂ and O₂, a few studies have used unfixed samples (only preserved dark at
597 +4°C) up to 48h after sampling to determine CO₂ or DIC concentrations (e.g., Sobek et al. 2003,
598 Kokic et al., 2015). So, the CO₂ and O₂ concentrations in the unfixed samples collected after 24h
599 incubation are the most representative of the initial real concentrations. Biological activity might have
600 had an impact, but this is likely negligible over the first 24h. In addition, the fact that the CO₂ and O₂
601 concentrations in the samples fixed with AgNO₃ after 24h, three weeks and three months are equal to
602 those from unfixed samples after 24h (Fig. 1) confirms that the unfixed samples after 24h can be used
603 as a control. In fact, only samples fixed with AgNO₃ are trustful given the expected toxicity of Ag, the
604 absence of impact on pH (Fig. 2), and unchanged concentrations over the three-month experiment for
605 all gases. Similarly, N₂O and N₂ concentrations in the unfixed samples after 24h can be used as
606 control. However, for CH₄, Fig. 1 shows that already after 24h, the CH₄ concentration in the unfixed
607 samples is below atmospheric saturation while it is consistently much higher in all three sets of fixed
608 samples. Boreal lakes are typically over saturated with respect to CH₄ (Valiente et al., 2022) and it is
609 very unlikely that CH₄ could have been produced in lake water incubated under high concentration of
610 oxygen and toxic preservatives. Hence, unfixed samples do not represent real CH₄ concentrations.
611 These observations are all consistent with the fact that the three preservatives were effective in
612 preserving CH₄ from oxidation. Even at t = 24h, preservatives are required to preserve CH₄ in oxic
613 samples. In fact, oxic methanotrophy typically show rates in the order of μM day⁻¹ (Thottathil et al.,

Formatted: Subscript

Formatted: Subscript

Formatted: Subscript

Formatted: Subscript

Formatted: Subscript

Formatted: Subscript

Formatted: Subscript

Formatted: Subscript

Formatted: Subscript

Formatted: Subscript

Formatted: Subscript

Formatted: Subscript

Formatted: Subscript

Formatted: Subscript

Formatted: Subscript

Formatted: Subscript

Formatted: Subscript

614 2019; van Grinsven et al., 2021). Hence, a CH₄ consumption of 0.3 μM within 24h in the unfixed
615 water samples is realistic (Fig. 1).

616 In summary, preservation with AgNO₃ is the only method that offered robust determination of all five
617 dissolved gases with negligible changes in concentration over time.

Formatted: Subscript

618 4.2 Risks of mis-estimating dissolved gas concentration with HgCl₂ and CuCl₂ preservation

Formatted: Subscript

619 Both sets of samples preserved with either HgCl₂ and CuCl₂ showed CO₂ concentrations that were
620 much higher than the unfixed (after 24h) or the AgNO₃-fixed samples. This is due to an acidification
621 of the poorly buffered (alkalinity 127 μM) and near neutral water (pH=6.73), shifting the carbonate
622 equilibrium from HCO₃⁻ to CO₂ as also shown by Borges et al. (2019). In fact, a rapid decrease in pH
623 was observed upon HgCl₂ and CuCl₂ amendments (Fig. 2). The increase of CO₂ from about 130 μM
624 to ~160 μM after 3 weeks in both sample sets preserved with HgCl₂ and CuCl₂ is not mirrored by a
625 similar decrease in O₂ (Fig. 1) This suggests that oxalic respiration is not the main source for this
626 additional 30 μM of CO₂ but rather points towards additional acidification of the samples caused, e.g.,
627 by kinetically controlled complexation of Hg²⁺ with dissolved organic matter (Miller et al., 2009). In
628 fact, the relatively slow complexation of Hg²⁺ with organic thiol groups can release two protons
629 (Skylberg, 2008) and up to three, with some participation of a third weak-acid group (Khwaja et al.,
630 2006). The transient nature of acidification caused by HgCl₂ and CuCl₂ is also evident in the pH
631 impacts showing higher acidification after 24h than after 2h incubation (Fig. 2). The following
632 decrease in CO₂ after 3 months (down to ~145 μM) points to other processes. The precipitation of Hg
633 and Cu carbonates, given their high saturation index values (Tab. 2), would be consistent with the
634 decrease in CO₂ concentrations observed between three weeks and three months. Calcite precipitation
635 is typically observed in supersaturated solutions within 48h (Kim et al., 2020). Hence, it is realistic to
636 consider that Hg and Cu carbonate precipitation influenced the CO₂ concentration within the
637 preserved samples over the three months of storage time. Impacts of Hg or Cu carbonate precipitation
638 is not evident after three weeks likely because of slow but persistent CO₂ production in presence of
639 HgCl₂ and CuCl₂ related to acidification as described above (Fig. 1). However, after three weeks, this
640 production likely weakens and is counterbalanced by increasing carbonate precipitation.

Formatted: Subscript

Formatted: Subscript

Formatted: Subscript

Formatted: Subscript

641 Overall, the addition of HgCl₂ or CuCl₂ following sampling increased CO₂ concentrations by 47%
642 within the first 24h compared to the unfixed consistent with the -0.16 to -0.21 pH-unit acidification
643 observed over the same time in the pH incubation experiment (Fig. 2) and the pH estimated with
644 PHREEQC without the interaction with dissolved organic matter (Tab. 2). In fact, introducing pH and
645 CO₂ concentration values of 6.40–6.45 and 130 μM, respectively, for the samples preserved with
646 HgCl₂ and CuCl₂ into Eqs. 1 and 2 yields DIC concentrations (C_T) of about 270 μM at t=24h. These
647 DIC concentrations are almost equal to those calculated for the unfixed samples and those preserved
648 with AgNO₃ at t = 24h, i.e., with a pH of 6.73 and CO₂ concentration of 88 μM. Interestingly, the

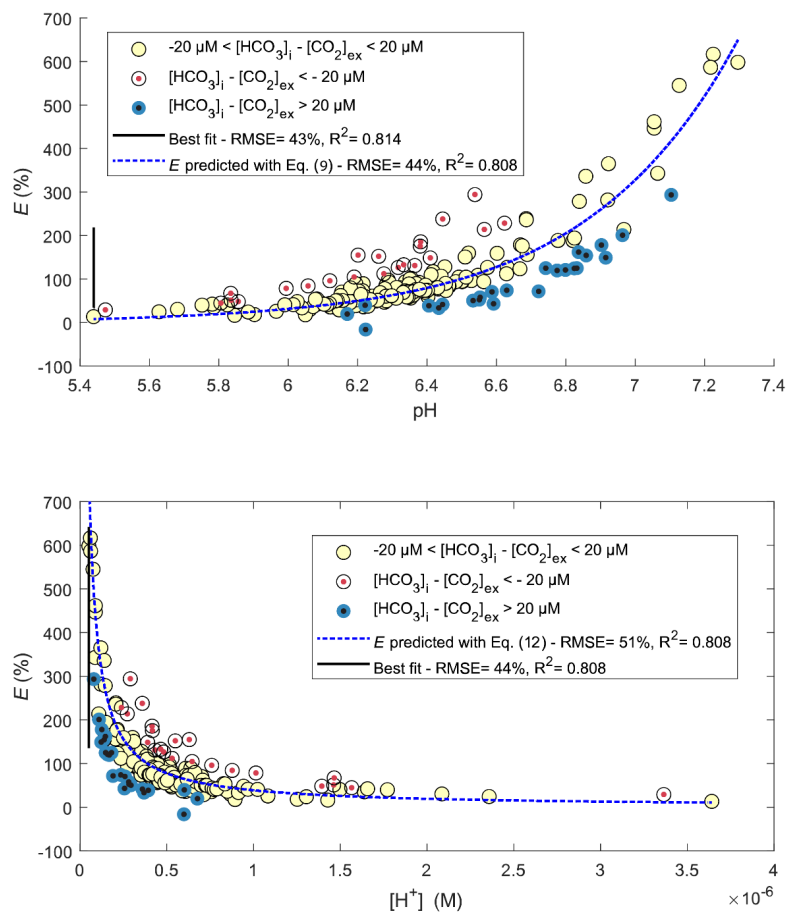
CO₂ overestimation from HgCl₂ fixation – Clayer et al.

649 concentration of CO₂ in the samples preserved with HgCl₂ and CuCl₂ continue to increase up to ~160
650 μM after 3 weeks. Given that oxic respiration is inhibited (Fig. 1), this additional CO₂ is believed to
651 originate from progressive release of protons following relatively slow complexation of Hg²⁺ with
652 dissolved organic matter (Khwaja et al., 2006; Miller et al., 2009; Skyllberg, 2008). Note that
653 PHREEQC could not predict complexation of Hg²⁺ with dissolved organic matter given that we
654 neglected the effect of dissolved organic matter.

655 Unlike the AgNO₃-fixed samples, all the other samples showed an initial increase in N₂O
656 concentration from 24h to 3 weeks, followed by a decrease from three weeks to 3 months. Similar
657 patterns of net N₂O production followed by net consumption were also reported in short-term
658 incubations of seawater from the high latitude Atlantic Ocean, although over much shorter timescales,
659 i.e., 48 and 96h (Rees et al., 2021). The large difference in kinetics between the latter experiment
660 (Rees et al., 2021) and our incubation might be attributable to differences in incubation temperature
661 where the seawater from the high latitude Atlantic Ocean was incubated at ambient temperatures
662 while our samples were kept at +4°C. Other difference in the experimental setup might have also
663 played a role. The lack of inhibition of N₂O production and consumption in the samples preserved
664 with HgCl₂ and CuCl₂ can be attributed to the fact that N₂O production tends to increase under
665 increasing acidic conditions (Knowles, 1982; Mørkved et al., 2007; Seitzinger, 1988). In fact, the
666 mole fraction of N₂O produced during denitrification increases compared to N₂ as pH decreases
667 (Knowles, 1982).

Formatted: Subscript

Formatted: Subscript



669

670 **Figure 34.** Comparison of observed (circles) and predicted (blue line) relative overestimation (E) of
 671 CO₂ concentrations caused by HgCl₂ fixation in Lake Lundebyvannet samples as a function of pH
 672 (top panel) or proton concentration (bottom panel). The black line shows the best fit of the regression
 673 analysis. White symbols represent samples for which the bicarbonate concentration in the unfixed
 674 samples ($[\text{HCO}_3^-]_i$) is nearly equal to CO₂ overestimation ($[\text{CO}_2]_{\text{ex}}$), i.e., $\pm 20 \mu\text{M}$ (equivalent to a pH
 675 error of 0.05), while red and blue symbols represent samples for which initial bicarbonate
 676 concentration was lower and higher than the CO₂ overestimation, respectively.

4.3 Using PHREEQC to estimate acidification caused by HgCl₂ in samples from Lake Lundebyvannet

As for the samples from Lake Svartkulp as described above, the overestimation of CO₂ concentration in the samples from Lake Lundebyvannet fixed with HgCl₂ (161 μM added; Fig. 3) likely stems from the acidification shifting the carbonate equilibrium from bicarbonate to CO₂. In fact, PHREEQC predicted a decrease of 0.6 to 1.8 units of pH related to HgCl₂ addition in these samples (Fig. S1).

The relative overestimation of CO₂ (*E* in Fig. 4) followed a typical exponential increase reflecting the decrease in absolute CO₂ concentration with increasing pH (Stumm & Morgan, 1981) caused here by phytoplankton photosynthesis. In fact, the exponential increase in CO₂ overestimation is easily predicted by Eq. (9) with an equivalent level of accuracy as the optimized exponential function (Fig. 4). Consistently, the relative overestimation of CO₂ (*E*) shows an inverse decrease with [H⁺] that is well reproduced by a simple inverse function ($3.25 \times 10^{-5} / [H^+]$; RMSE=44%, R²=0.81, p<0.0001; Fig. 4) and predicted by Eq. (15), with an α value of 1. Combining Eqs. 8 and 15 and solving it with pH values estimated from PHREEQC (Fig. S1) for α yields values ranging between 0.72 and 0.89 with an average of 0.85. Unexpectedly, this average α value is almost equal to the ratio of the inverse function coefficient and K₁, i.e., $\frac{3.25 \times 10^{-5}}{K_1} = 0.87$. Hence, the relative overestimation of CO₂ (*E*) caused by HgCl₂ fixation is easily predicted by the change in bicarbonate equilibrium knowing the proton release from HgCl₂ addition, here estimated with PHREEQC.

Hence, PHREEQC can be used to predict decrease in pH caused by HgCl₂ fixation, if sufficient knowledge is gathered on the ionic water composition. Proton release during HgCl₂ fixation can be represented by the following reaction:



From reaction 2, it becomes evident that the initial concentration of chloride in the water samples will likely limit HgCl₂ dissociation and proton release. This is a likely mechanism occurring in seawater where HgCl₂ has been shown to cause a decrease in pH, although at a negligible level with a maximum decrease in pH of -0.01 (Chou et al., 2016).

Figure 32 shows that a range of water samples were associated with a relative CO₂ overestimation (*E*) that substantially deviated from the overestimation predicted with Eq. 142 (red and blue symbols in Fig. 34). In fact, some samples had a higher initial bicarbonate content ([HCO₃⁻]_i) than the excess CO₂ concentration ([CO₂]_{ex}), while other showed the opposite. The former case (blue symbols in Fig. 34) can easily be explained by a higher buffering capacity of the sampled water, i.e., a higher pH after HgCl₂-fixation than that predicted by PHREEQC related to a different water composition. Indeed, the concentration of major elements in the water from Lake Lundebyvannet may vary significantly over time, and in absence of data, we considered that the water composition, except for DIC, pH and

Formatted: Subscript

Formatted: Subscript

Formatted: Subscript

Formatted: Subscript

Formatted: Subscript

Formatted: Subscript

Formatted: Font: Italic

Formatted: Subscript

Formatted: Subscript

710 HgCl₂, was constant over time. By contrast, samples associated with $[CO_2]_{ex}$ being larger than
711 $[HCO_3^-]_i$ are more enigmatic. In order to shed light on possible explanations, we visually inspected
712 trends between empirical deviations from predictions, i.e., residuals, and *in situ* temperature or pH.
713 Absolute values of residuals showed a progressive increase with pH and *in situ* temperature which is
714 in agreement with decreasing precision of the headspace method with increasing temperature and pH
715 (Koschorreck et al., 2021). In fact, CO₂ is less soluble at higher temperature, hence more gas can
716 evade during sampling, and thus the error increases with *in situ* temperature. In addition, at higher pH,
717 CO₂ concentration decreases and consequently the absolute error on CO₂ quantification becomes
718 larger relative to measured CO₂ concentration. Interestingly, many of the high residual values were
719 not evenly distributed across the year, nor across the summer and were rather associated with only a
720 few specific sampling events during summer (Fig. S2). This suggests that ~~degassing gas loss~~ could
721 have occurred due to high ambient temperature in the field. Water associated with $[CO_2]_{ex}$ being
722 larger than $[HCO_3^-]_i$ (red symbols in Fig. 43 and S4) could have been subject to a larger ~~degassing gas~~
723 ~~loss~~ in the samples collected for DIC analysis than the samples for GC analysis. On the other hand,
724 ~~degassing loss of gas~~ was likely larger for samples for GC analysis than for DIC analysis for water
725 associated with $[HCO_3^-]_i$ being larger than $[CO_2]_{ex}$ (blue symbols in Fig. 43 and Fig. S2). In addition
726 to ~~degassing gas losses~~ and temperature effects, errors in pH measurements can also cause a large
727 misestimation of CO₂ concentration from DIC analysis, and this error increases exponentially with pH
728 following the shift in carbonate equilibrium. In summary, our analysis is consistent with that of
729 Koschorreck et al. (2021) showing that errors in the determination of CO₂ concentrations are smaller
730 at lower pH and lower temperature (Fig. S2).

731 34.44. Implications for the estimation of lake and reservoir C cycling and recommendations
732 Using HgCl₂ (or CuCl₂) to preserve dissolved gas samples in poorly buffered water samples ~~would~~
733 ~~have~~ large impacts on CO₂ concentrations with considerable risk of leading to incorrect
734 interpretations. The risk of mis-estimating CO₂ concentration due to HgCl₂ and CuCl₂ preservation is
735 the highest when natural water pH is close to the first carbonic acid dissociation constant ($pK_1 = 6.41$
736 at 25°C; Stumm & Morgan, 1996). It implies that any small shift in pH will have a significant impact
737 in the carbonate equilibrium between bicarbonate to CO₂. The risk is also the highest in the lowest
738 ionic strength waters. In that respect, low-ionic strength, slightly acidic to neutral, moderately humic
739 lakes commonly found in Norway (de Wit et al., 2023), large parts of Sweden (Valina et al. 2014),
740 and Finland, Atlantic Canada (Houle et al., 2022), Ontario, Québec, and North-East USA (Skjelkvåle
741 and de Wit 2011; Weyhenmeyer et al., 2019) are the most prone to errors in CO₂ concentrations
742 related to HgCl₂ or CuCl₂ preservation. A significant part of these low-ionic strength lakes become
743 increasingly sensitive to changes in nutrients with strong impacts on their role in carbon cycling
744 (Myrstener et al., 2022). In this context, it is crucial to avoid mis-estimation of CO₂ concentrations
745 and thus avoid use of HgCl₂ or CuCl₂ to ensure a robust understanding of the role of autotrophic

Formatted: Subscript

Formatted: Subscript

Formatted: Subscript

Formatted: Subscript

Formatted: Subscript

Formatted: Subscript

CO₂ overestimation from HgCl₂ fixation – Clayer et al.

746 processes in lake C cycling. Below we describe the implications for the lake C budget of
747 Lundebyvannet as an example of a mis-estimation of the role of photosynthesis in a typical productive
748 boreal lake.

749 ~~In fact~~In Lake Lundebyvannet, over the ice-free season, average CO₂ concentrations ~~in Lake~~
750 Lundebyvannet determined following HgCl₂-fixation and GC analysis were 82% higher than those
751 obtained from DIC analyses (~~Table-Tab.~~ 3; Fig. 4~~5~~ and S3). CO₂ concentrations obtained from HgCl₂-
752 fixed samples created the illusion that Lake Lundebyvannet was a steady net source of CO₂ to the
753 atmosphere over the ice-free season with large CO₂ saturation deficit (Fig. 3) while, in reality, the lake
754 switched from being a net source in May, to a net sink over a few weeks in June, and returning to a
755 net source in July (Fig. 4~~5~~ and S3). Indeed, monthly CO₂ overestimation related to HgCl₂-fixation
756 reached about 300% in June (~~Table-Tab.~~ 3). Propagating this overestimation into the estimates of CO₂
757 diffusion fluxes with typical wind-based models yields overestimation of CO₂ fluxes of 108–112%
758 over the ice-free season and up to 2100% in June (~~Tables-Tab.~~ 3 and S3). Hence, interpreting CO₂
759 data without correcting for CO₂ overestimation caused by HgCl₂-fixation leads to negligence of the
760 role of photosynthesis in lake C cycling with major implications for current and future predictions of
761 lake CO₂ emissions.

762 The use of HgCl₂ to preserve water samples prior to dissolved gas analyses is part of the current
763 guidelines for greenhouse gas measurements in freshwater reservoirs (Machado Damazio et al., 2012;
764 UNESCO/IHA, 2008, 2010). Hence, there is a risk of overestimating CO₂ concentrations and
765 emissions, in absence of discrete measurement of emissions, from hydropower reservoirs with
766 consequence on the present and expected greenhouse gas footprint from hydroelectricity. To ensure
767 precise estimation of greenhouse concentration and, possibly, emission from hydropower, the use of
768 HgCl₂ should therefore be discontinued.

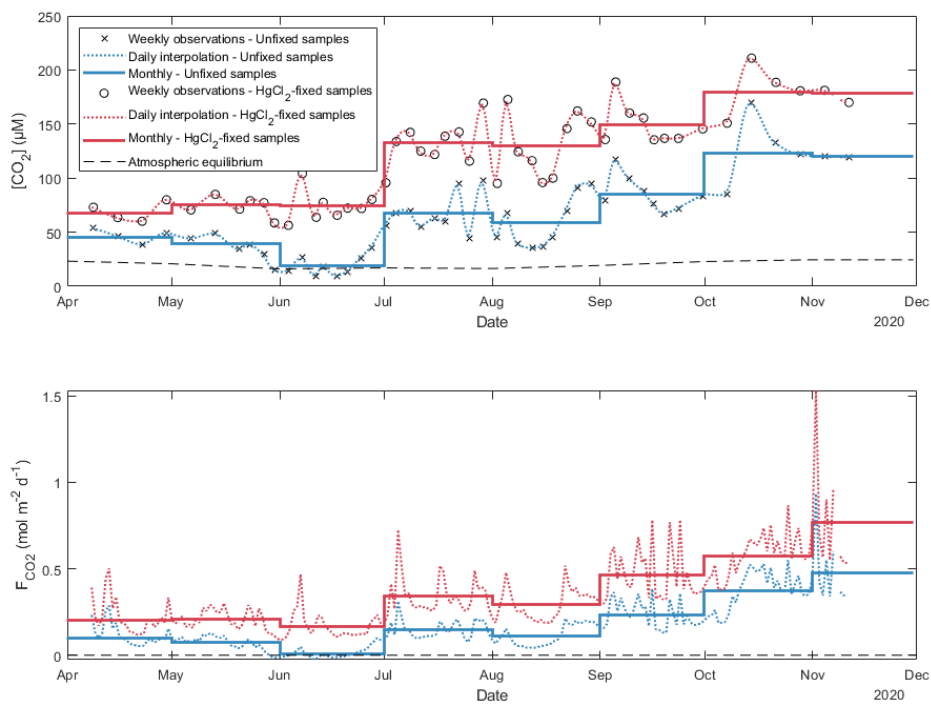
769 5. Conclusion

770 Mercury is a potent neurotoxin for humans and toxic for the environment and its use should be
771 discouraged, notably following the Minamata convention on mercury, a global treaty ratified by 126
772 countries (16 December 2020) to protect human health and the environment from the adverse effects
773 of mercury. This study further questions the use of HgCl₂ for preservation of poorly buffered (low
774 ionic strength) water samples with high DOC concentration for analysis of dissolved gases in the
775 laboratory. Although CuCl₂ is less toxic, it behaved similarly to HgCl₂ and cannot be recommend. In
776 fact, both chlorinated inhibitors caused a significant decrease in pH shifting the carbonate equilibrium
777 towards CO₂ and are also suspected to promote carbonate precipitation over long-term storage. The
778 only promising inhibitor tested in this study was AgNO₃ notably for dissolved CO₂, CH₄ and N₂O.
779 Silver nitrate ~~may be~~is a suitable substitute for HgCl₂ in low-ionic strength waters, ~~but~~ further tests
780 should be carried out with a range of inhibitor concentration and more diverse water samples. The use

CO₂ overestimation from HgCl₂ fixation – Clayer et al.

781 of chemical inhibitors may not be the best approach. Alternatives exist, such as directly measuring gas
782 concentrations *in situ* with sensors, or sampling the headspace out in the field, and bringing back gas
783 samples (e.g., Cole et al., 1994; Karlsson et al., 2013; Kling et al., 1991; Valiente et al., 2022), rather
784 than water samples, to the lab for gas chromatography analyses. However, care must be taken to know
785 the exact equilibration temperature (Koschorreck et al., 2021) and to avoid gas exchange with the
786 atmosphere as well as to use a clean background gas during headspace equilibration which can be
787 challenging in remote environments under harsh meteorological conditions.

CO₂ overestimation from HgCl₂ fixation – Clayer et al.



788

789 **Figure 54.** Daily and monthly surface CO₂ concentrations ([CO₂]; top panel) and diffusion fluxes
790 (F_{CO₂}; bottom panel) at the water-atmosphere interface from Lake Lundebyvannet ([also in Tab. 3](#)).
791 Unfixed samples were obtained by DIC analysis. Daily [CO₂] was interpolated from weekly data
792 using a modified spline (see text for details). Diffusion fluxes were calculated following Cole &
793 Caraco (1998).

CO₂ overestimation from HgCl₂ fixation – Clayer et al.

794 We further advise against interpretation of CO₂ concentration data from low ionic strength, circum-
795 neutral water samples preserved with HgCl₂ or CuCl₂. The overestimation of CO₂ concentration
796 caused by HgCl₂ can mask the effect of photosynthesis on lake carbon balance, creating the illusion
797 that lakes are net CO₂ sources when they are net CO₂ sinks. Our analysis from Lake Lundebyvannet
798 shows that HgCl₂ fixation led to an overestimation of the CO₂ concentration by a factor of 1.8, on
799 average, but approaching a factor of 4 during the peak photosynthetic period. An even larger impact is
800 expected on CO₂ diffusive fluxes which were overestimated by a factor of 2 on average and up to a
801 factor of >20 during peak photosynthesis. Interpreting such data would have underestimated the
802 current and future role of aquatic photosynthesis.

803 **Data availability**

804 All data supporting this study will be made available on a permanent repository upon acceptance, e.g.,
805 Hydroshare.

806 **Author contribution**

807 JET, AK, and TR supervised and PD, KN and FC contributed to the study design. JET, KN and TR
808 carried out the experiments. PD and TR performed the chemical analyses. JET and FC wrote the first
809 draft. FC performed the modelling, data, and statistical analyses, and drafted the figures. All co-
810 authors edited the manuscript.

811 **Competing interests**

812 The contact author has declared that none of the authors has any competing interests.

813 **Acknowledgements**

814 We are grateful to Benoît Demars for research assistance, coordination, and useful comments and
815 discussions on an earlier version of this manuscript and to Heleen de Wit for discussions. Research
816 was funded by NIVA and through the Global Change at Northern Latitude (NoLa) project #200033.

817

818 **References**

- 819 Akima, H. (1974). A method of bivariate interpolation and smooth surface fitting based on local
820 procedures. *Communications of the ACM*, 17(1), 18–20.
821 <https://doi.org/10.1145/360767.360779>
- 822 Allison, J., Brown, D., & Novo-Gradac, K. (1991). *MINTEQA2/PRODEFA2, a geochemical*
823 *assessment model for environmental systems: Version 3. 0 user's manual*. GA: US
824 Environmental Protection Agency.
- 825 [Amorim, M. J. B., & Scott-Fordsmand, J. J. \(2012\). Toxicity of copper nanoparticles and CuCl₂ salt](#)
826 [to *Enchytraeus albidus* worms: Survival, reproduction and avoidance responses.](#)
827 [*Environmental Pollution*, 164, 164–168. <https://doi.org/10.1016/j.envpol.2012.01.015>](#)

Formatted: French (France)

- 828 Borges, A. V., Darchambeau, F., Lambert, T., Morana, C., Allen, G. H., Tambwe, E., Toengaho
 829 Sembaito, A., Mambo, T., Nlandu Wabakhangazi, J., Descy, J.-P., Teodoru, C. R., &
 830 Bouillon, S. (2019). Variations in dissolved greenhouse gases (CO₂, CH₄, N₂O) in the Congo
 831 River network overwhelmingly driven by fluvial-wetland connectivity. *Biogeosciences*,
 832 *16*(19), 3801–3834. <https://doi.org/10.5194/bg-16-3801-2019>
- 833 Carroll J.J., Slupsky J.D. & Mather A.E. (1991) The solubility of carbon dioxide in water at low
 834 pressure. *Journal of Physical and Chemical Reference Data*, **20**, 1201-1209.
 835 <https://doi.org/10.1063/1.555900>
- 836 Chen, C. Y., Driscoll, C., Eagles-Smith, C. A., Eckley, C. S., Gay, D. A., Hsu-Kim, H., Keane, S. E.,
 837 Kirk, J. L., Mason, R. P., Obrist, D., Selin, H., Selin, N. E., & Thompson, M. R. (2018). A
 838 Critical Time for Mercury Science to Inform Global Policy. *Environmental Science &*
 839 *Technology*, *52*(17), 9556–9561. <https://doi.org/10.1021/acs.est.8b02286>
- 840 Chen H., Johnston R.C., Mann B.F., Chu R.K., Tolic N., Parks J.M. & Gu B. (2017) Identification of
 841 mercury and dissolved organic matter complexes using ultrahigh resolution mass
 842 spectrometry. *Environmental Science & Technology Letters*, **4**, 59-65.
 843 <https://doi.org/10.1021/acs.estlett.6b00460>
- 844 Chou W.C., Gong G.C., Yang C.Y. & Chuang K.Y. (2016) A comparison between field and
 845 laboratory pH measurements for seawater on the East China Sea shelf. *Limnology and*
 846 *Oceanography-Methods*, **14**, 315-322. <https://doi.org/10.1002/lom3.10091>
- 847 Ciavatta L. & Grimaldi M. (1968) The hydrolysis of mercury(II) chloride, HgCl₂. *Journal of*
 848 *Inorganic and Nuclear Chemistry*, **30**, 563-581. [https://doi.org/10.1016/0022-1902\(68\)80483-
 849 *X*](https://doi.org/10.1016/0022-1902(68)80483-X)
- 850 Clayer, F., Thrane, J.-E., Brandt, U., Dörsch, P., & de Wit, H. A. (2021). Boreal Headwater
 851 Catchment as Hot Spot of Carbon Processing From Headwater to Fjord. *Journal of*
 852 *Geophysical Research: Biogeosciences*, *126*(12), e2021JG006359.
 853 <https://doi.org/10.1029/2021JG006359>
- 854 Cole, J. J., Caraco, N. F., Kling, G. W., & Kratz, T. K. (1994). Carbon Dioxide Supersaturation in the
 855 Surface Waters of Lakes. *Science*, *265*(5178), Article 5178.
 856 <https://doi.org/10.1126/science.265.5178.1568>
- 857 Cole, J. J., & Caraco, N. F. (1998). Atmospheric exchange of carbon dioxide in a low-wind
 858 oligotrophic lake measured by the addition of SF₆. *Limnology and Oceanography*, *43*(4),
 859 Article 4. <https://doi.org/10.4319/lo.1998.43.4.0647>
- 860 Crusius, J., & Wanninkhof, R. (2003). Gas transfer velocities measured at low wind speed over a lake.
 861 *Limnology and Oceanography*, *48*(3), Article 3. <https://doi.org/10.4319/lo.2003.48.3.1010>
- 862 Deheyn, D. D., Bencheikh-Latmani, R., & Latz, M. I. (2004). Chemical speciation and toxicity of
 863 metals assessed by three bioluminescence-based assays using marine organisms.
 864 *Environmental Toxicology*, *19*(3), 161–178. <https://doi.org/10.1002/tox.20009>
- 865 de Wit, H. A., Garmo, Ø. A., Jackson-Blake, L. A., Clayer, F., Vogt, R. D., Austnes, K., Kaste, Ø.,
 866 Gundersen, C. B., Guerrero, J. L., & Hindar, A. (2023). Changing Water Chemistry in One
 867 Thousand Norwegian Lakes During Three Decades of Cleaner Air and Climate Change.
 868 *Global Biogeochemical Cycles*, *37*(2), e2022GB007509.
 869 <https://doi.org/10.1029/2022GB007509>
- 870 Dickson A.G., Sabine C.L. & Christian J.R. (2007) *Guide to best practices for ocean CO₂*
 871 *measurements*, North Pacific Marine Science Organization.
- 872 Duan, Z., & Mao, S. (2006). A thermodynamic model for calculating methane solubility, density and
 873 gas phase composition of methane-bearing aqueous fluids from 273 to 523K and from 1 to
 874 2000bar. *Geochimica et Cosmochimica Acta*, *70*(13), Article 13.
 875 <https://doi.org/10.1016/j.gca.2006.03.018>
- 876 Foti C., Giuffrè O., Lando G. & Sammartano S. (2009) Interaction of inorganic mercury (II) with
 877 polyamines, polycarboxylates, and amino acids. *Journal of Chemical & Engineering Data*,
 878 **54**, 893-903. <https://doi.org/10.1021/jc800685c>
- 879 *Frost API*. (2022). <https://frost.met.no/index.html>
- 880 Guérin, F., Abril, G., Richard, S., Burbán, B., Reynouard, C., Seyler, P., & Delmas, R. (2006).
 881 Methane and carbon dioxide emissions from tropical reservoirs: Significance of downstream
 882 rivers. *Geophysical Research Letters*, *33*(21). <https://doi.org/10.1029/2006GL027929>

- 883 Guérin, F., Abril, G., Serça, D., Delon, C., Richard, S., Delmas, R., Tremblay, A., & Varfalvy, L.
 884 (2007). Gas transfer velocities of CO₂ and CH₄ in a tropical reservoir and its river
 885 downstream. *Journal of Marine Systems*, 66(1), Article 1.
 886 <https://doi.org/10.1016/j.jmarsys.2006.03.019>
- 887 Halmi, M. I. E., Kassim, A., & Shukor, M. Y. (2019). Assessment of heavy metal toxicity using a
 888 luminescent bacterial test based on *Photobacterium* sp. Strain MIE. *Rendiconti Lincei. Scienze*
 889 *Fisiche e Naturali*, 30(3), 589–601. <https://doi.org/10.1007/s12210-019-00809-5>
- 890 [Hagman, C. H. C., Ballot, A., Hjerermann, D. Ø., Skjelbred, B., Brettum, P., & Ptacnik, R. \(2015\). The](#)
 891 [occurrence and spread of *Gonyostomum semen* \(Ehr.\) Diesing \(Raphidophyceae\) in](#)
 892 [Norwegian lakes. *Hydrobiologia*, 744\(1\), 1–14. <https://doi.org/10.1007/s10750-014-2050-y>](#)
- 893 Hamme R.C. & Emerson S.R. (2004) The solubility of neon, nitrogen and argon in distilled water and
 894 seawater. *Deep-Sea Research Part I-Oceanographic Research Papers*, 51, 1517-1528.
 895 <https://doi.org/10.1016/j.dsr.2004.06.009>
- 896 Hassen A., Saidi N., Cherif M. & Boudabous A. (1998) Resistance of environmental bacteria to heavy
 897 metals. *Bioresource technology*, 64, 7-15. [https://doi.org/10.1016/S0960-8524\(97\)00161-2](https://doi.org/10.1016/S0960-8524(97)00161-2)
- 898 Hessen, D. O., Håll, J. P., Thrane, J.-E., & Andersen, T. (2017). Coupling dissolved organic carbon,
 899 CO₂ and productivity in boreal lakes. *Freshwater Biology*, 62(5), 945–953.
 900 <https://doi.org/10.1111/fwb.12914>
- 901 Hilgert, S., Scapulatempo Fernandes, C. V., & Fuchs, S. (2019). Redistribution of methane emission
 902 hot spots under drawdown conditions. *Science of The Total Environment*, 646, 958–971.
 903 <https://doi.org/10.1016/j.scitotenv.2018.07.338>
- 904 Horvatić J. & Peršić V. (2007) The effect of Ni²⁺, Co²⁺, Zn²⁺, Cd²⁺ and Hg²⁺ on the growth
 905 rate of marine diatom *Phaeodactylum tricornutum* Bohlin: microplate growth inhibition test.
 906 *Bulletin of Environmental Contamination and Toxicology*, 79, 494-498.
 907 <https://doi.org/10.1007/s00128-007-9291-7>
- 908 [Houle, D., Augustin, F., & Couture, S. \(2022\). Rapid improvement of lake acid–base status in](#)
 909 [Atlantic Canada following steep decline in precipitation acidity. *Canadian Journal of*](#)
 910 [Fisheries and Aquatic Sciences, 79\(12\), 2126–2137. <https://doi.org/10.1139/cjfas-2021-0349>](#)
- 911 IEA. (2020). *Key World Energy Statistics 2020*. IEA, International Energy Agency.
 912 <https://www.iea.org/reports/key-world-energy-statistics-2020>
- 913 Karlsson, J., Giesler, R., Persson, J., & Lundin, E. (2013). High emission of carbon dioxide and
 914 methane during ice thaw in high latitude lakes. *Geophysical Research Letters*, 40(6), Article
 915 6. <https://doi.org/10.1002/grl.50152>
- 916 Khwaja, A. R., Bloom, P. R., & Brezonik, P. L. (2006). Binding Constants of Divalent Mercury
 917 (Hg²⁺) in Soil Humic Acids and Soil Organic Matter. *Environmental Science & Technology*,
 918 40(3), 844–849. <https://doi.org/10.1021/es051085c>
- 919 Kim, D., Mahabadi, N., Jang, J., & van Paassen, L. A. (2020). Assessing the Kinetics and Pore-Scale
 920 Characteristics of Biological Calcium Carbonate Precipitation in Porous Media using a
 921 Microfluidic Chip Experiment. *Water Resources Research*, 56(2), e2019WR025420.
 922 <https://doi.org/10.1029/2019WR025420>
- 923 Kling, G. W., Kipphut, G. W., & Miller, M. C. (1991). Arctic Lakes and Streams as Gas Conduits to
 924 the Atmosphere: Implications for Tundra Carbon Budgets. *Science*, 251(4991), 298–301.
 925 <https://doi.org/10.1126/science.251.4991.298>
- 926 Knowles, R. (1982). Denitrification. *Microbiological Reviews*, 46(1), 43–70.
 927 <https://doi.org/10.1128/mr.46.1.43-70.1982>
- 928 [Kokic, J., Wallin, M. B., Chmiel, H. E., Denfeld, B. A., & Sobek, S. \(2015\). Carbon dioxide evasion](#)
 929 [from headwater systems strongly contributes to the total export of carbon from a small boreal](#)
 930 [lake catchment. *Journal of Geophysical Research: Biogeosciences*, 120\(1\), 13–28.](#)
 931 <https://doi.org/10.1002/2014JG002706>
- 932 Koschorreck, M., Prairie, Y. T., Kim, J., & Marcé, R. (2021). Technical note: CO₂ is not like CH₄ –
 933 limits of and corrections to the headspace method to analyse pCO₂ in fresh water.
 934 *Biogeosciences*, 18(5), 1619–1627. <https://doi.org/10.5194/bg-18-1619-2021>
- 935 Larrañaga, M., Lewis, R., & Lewis, R. (2016). Hawley's Condensed Chemical Dictionary, Sixteenth
 936 Edition. i–xiii. <https://doi.org/10.1002/9781119312468.fmatter>

Formatted: Norwegian (Bokmål)

- 937 Liang X., Lu X., Zhao J., Liang L., Zeng E.Y. & Gu B. (2019) Stepwise reduction approach reveals
 938 mercury competitive binding and exchange reactions within natural organic matter and mixed
 939 organic ligands. *Environmental Science & Technology*, **53**, 10685-10694.
 940 <https://doi.org/10.1021/acs.est.9b02586>
- 941 Machado Damazio, J., Cordeiro Geber de Melo, A., Piñeiro Maceira, M. E., Medeiros, A., Negrini,
 942 M., Alm, J., Schei, T. A., Tateda, Y., Smith, B., & Nielsen, N. (2012). *Guidelines for*
 943 *quantitative analysis of net GHG emissions from reservoirs: Volume 1: Measurement*
 944 *Programmes and Data Analysis*. International Energy Agency (IEA).
 945 https://www.ieahydro.org/media/992f6848/GHG_Guidelines_22October2012_Final.pdf
- 946 Magen, C., Lapham, L. L., Pohlman, J. W., Marshall, K., Bosman, S., Casso, M., & Chanton, J. P.
 947 (2014). A simple headspace equilibration method for measuring dissolved methane.
 948 *Limnology and Oceanography: Methods*, **12**(9), 637–650.
 949 <https://doi.org/10.4319/lom.2014.12.637>
- 950 Miller, C. L., Southworth, G., Brooks, S., Liang, L., & Gu, B. (2009). Kinetic Controls on the
 951 Complexation between Mercury and Dissolved Organic Matter in a Contaminated
 952 Environment. *Environmental Science & Technology*, **43**(22), 8548–8553.
 953 <https://doi.org/10.1021/es901891t>
- 954 Millero F.J., Huang F. & Laferiere A.L. (2002) Solubility of oxygen in the major sea salts as a
 955 function of concentration and temperature. *Marine Chemistry*, **78**, 217-230.
 956 [https://doi.org/10.1016/S0304-4203\(02\)00034-8](https://doi.org/10.1016/S0304-4203(02)00034-8)
- 957 [Myrstener, M., Fork, M. L., Bergström, A.-K., Puts, I. C., Hauptmann, D., Isles, P. D. F., Burrows, R.](#)
 958 [M., & Sponseller, R. A. \(2022\). Resolving the Drivers of Algal Nutrient Limitation from](#)
 959 [Boreal to Arctic Lakes and Streams. *Ecosystems*, 25\(8\), 1682–1699.](#)
 960 <https://doi.org/10.1007/s10021-022-00759-4>
- 961 Mørkved, P. T., Dörsch, P., & Bakken, L. R. (2007). The N₂O product ratio of nitrification and its
 962 dependence on long-term changes in soil pH. *Soil Biology and Biochemistry*, **39**(8), 2048–
 963 2057. <https://doi.org/10.1016/j.soilbio.2007.03.006>
- 964 NILU. (2022). *EBAS*. <https://ebas-data.nilu.no/Default.aspx>
- 965 Nowack, B., Krug, H. F., & Height, M. (2011). 120 Years of Nanosilver History: Implications for
 966 Policy Makers. *Environmental Science & Technology*, **45**(4), 1177–1183.
 967 <https://doi.org/10.1021/es103316q>
- 968 NPIRS. (2023). *Purdue University*. <https://www.npirs.org/public>
- 969 Okuku, E. O., Bouillon, S., Tole, M., & Borges, A. V. (2019). Diffusive emissions of methane and
 970 nitrous oxide from a cascade of tropical hydropower reservoirs in Kenya. *Lakes &*
 971 *Reservoirs: Science, Policy and Management for Sustainable Use*, **24**(2), 127–135.
 972 <https://doi.org/10.1111/lre.12264>
- 973 Parkhurst, D. L., & Appelo, C. A. J. (2013). *Description of input and examples for PHREEQC version*
 974 *3—A computer program for speciation, batch-reaction, one-dimensional transport, and*
 975 *inverse geochemical calculations: U.S. Geological Survey Techniques and Methods* (book 6,
 976 chap. A43; p. 497). USGS. <http://pubs.usgs.gov/tm/06/a43/>
- 977 Powell K.J., Brown P.L., Byrne R.H., Gajda T., Hefter G., Sjöberg S. & Wanner H. (2004) Chemical
 978 speciation of Hg (II) with environmental inorganic ligands. *Australian Journal of Chemistry*,
 979 **57**, 993-1000. <https://doi.org/10.1071/CH04063>
- 980 Rai L.C., Gaur J.P. & Kumar H.D. (1981) Phycology and heavy-metal pollution. *Biological Reviews*,
 981 **56**, 99-151. <https://doi.org/10.1111/j.1469-185X.1981.tb00345.x>
- 982 [Ratte, H. T. \(1999\). Bioaccumulation and toxicity of silver compounds: A review. *Environmental*](#)
 983 [Toxicology and Chemistry, **18**\(1\), 89–108. <https://doi.org/10.1002/etc.5620180112>](#)
- 984 Rees, A. P., Brown, I. J., Jayakumar, A., Lessin, G., Somerfield, P. J., & Ward, B. B. (2021).
 985 Biological nitrous oxide consumption in oxygenated waters of the high latitude Atlantic
 986 Ocean. *Communications Earth & Environment*, **2**(1), Article 1.
 987 <https://doi.org/10.1038/s43247-021-00104-y>
- 988 [Rippner, D. A., Margenot, A. J., Fakra, S. C., Aguilera, L. A., Li, C., Sohng, J., Dynarski, K. A.,](#)
 989 [Waterhouse, H., McElroy, N., Wade, J., Hind, S. R., Green, P. G., Peak, D., McElrone, A. J.,](#)
 990 [Chen, N., Feng, R., Scow, K. M., & Parikh, S. J. \(2021\). Microbial response to copper oxide](#)

- 991 [nanoparticles in soils is controlled by land use rather than copper fate. *Environmental*](#)
 992 [Science: Nano](#), 8(12), 3560–3576. <https://doi.org/10.1039/D1EN00656H>
- 993 Rohrlack T., Frostad P., Riise G. & Hagman C.H.C. (2020) Motile phytoplankton species such as
 994 *Gonyostomum* semen can significantly reduce CO₂ emissions from boreal lakes.
 995 *Limnologia*, 84, 125810. <https://doi.org/10.1016/j.limno.2020.125810>
- 996 Schubert, C. J., Diem, T., & Eugster, W. (2012). Methane Emissions from a Small Wind Shielded
 997 Lake Determined by Eddy Covariance, Flux Chambers, Anchored Funnels, and Boundary
 998 Model Calculations: A Comparison. *Environmental Science & Technology*, 46(8), 4515–
 999 4522. <https://doi.org/10.1021/es203465x>
- 1000 Seitzinger, S. P. (1988). Denitrification in freshwater and coastal marine ecosystems: Ecological and
 1001 geochemical significance. *Limnology and Oceanography*, 33(4part2), 702–724.
 1002 <https://doi.org/10.4319/lo.1988.33.4part2.0702>
- 1003 Silver S. & Phung L.T. (2005) A bacterial view of the periodic table: genes and proteins for toxic
 1004 inorganic ions. *Journal of Industrial Microbiology & Biotechnology*, 32, 587–605.
 1005 <https://doi.org/10.1007/s10295-005-0019-6>
- 1006 [Skjelkvåle, B. L., & de Wit, H. A. \(2011\). Trends in precipitation chemistry, surface water chemistry](#)
 1007 [and aquatic biota in acidified areas in Europe and North America from 1990 to 2008 \(ICP](#)
 1008 [Waters report 106/2011\). In 126. Norsk institutt for vannforskning.](#)
 1009 <https://niva.brage.unit.no/niva-xmlui/handle/11250/215591>
- 1010 Skyllberg, U. (2008). Competition among thiols and inorganic sulfides and polysulfides for Hg and
 1011 MeHg in wetland soils and sediments under suboxic conditions: Illumination of controversies
 1012 and implications for MeHg net production. *Journal of Geophysical Research: Biogeosciences*, 113(G2). <https://doi.org/10.1029/2008JG000745>
- 1013 [Sobek, S., Algesten, G., Bergström, A.-K., Jansson, M., & Tranvik, L. J. \(2003\). The catchment and](#)
 1014 [climate regulation of pCO₂ in boreal lakes. *Global Change Biology*, 9\(4\), 630–641.](#)
 1015 <https://doi.org/10.1046/j.1365-2486.2003.00619.x>
- 1016 Stumm W. & Morgan J.J. (1981) *Aquatic Chemistry. An introduction emphasizing chemical*
 1017 *equilibria in natural waters*, Wiley Interscience, New York.
- 1018 Stumm, W., & Morgan, J. J. (1996). *Aquatic chemistry: Chemical equilibria and rates in natural*
 1019 *waters* (3rd ed.). Wiley.
- 1020 Taipale S.J. & Sonninen E. (2009) The influence of preservation method and time on the delta C-13
 1021 value of dissolved inorganic carbon in water samples. *Rapid Communications in Mass*
 1022 *Spectrometry*, 23, 2507–2510. <https://doi.org/10.1002/rcm.4072>
- 1023 Takahashi H.A., Handa H., Sugiyama A., Matsushita M., Kondo M., Kimura H. & Tsujimura M.
 1024 (2019) Filtration and exposure to benzalkonium chloride or sodium chloride to preserve water
 1025 samples for dissolved inorganic carbon analysis. *Geochemical Journal*, 53, 305–318.
 1026 <https://doi.org/10.2343/geochemj.2.0570>
- 1027 Thottathil, S. D., Reis, P. C. J., & Prairie, Y. T. (2019). Methane oxidation kinetics in northern
 1028 freshwater lakes. *Biogeochemistry*, 143(1), Article 1. <https://doi.org/10.1007/s10533-019-00552-x>
- 1029 Tipping E. (2007) Modelling the interactions of Hg(II) and methylmercury with humic substances
 1030 using WHAM/Model VI. *Applied Geochemistry*, 22, 1624–1635.
- 1031 Tørseth, K., Aas, W., Breivik, K., Fjæraa, A. M., Fiebig, M., Hjellbrekke, A. G., Lund Myhre, C.,
 1032 Solberg, S., & Yttri, K. E. (2012). Introduction to the European Monitoring and Evaluation
 1033 Programme (EMEP) and observed atmospheric composition change during
 1034 1972–2009. *Atmospheric Chemistry and Physics*, 12(12), 5447–5481.
 1035 <https://doi.org/10.5194/acp-12-5447-2012>
- 1036 Ullmann, F., Gerhartz, W., Yamamoto, Y. S., Campbell, F. T., Pfefferkorn, R., & Rounsaville, J. F.
 1037 (1985). Ullmann's encyclopedia of industrial chemistry (5th, completely rev. ed ed.). VCH.
- 1038 UNESCO/IHA. (2008). *Assessment of the GHG status of freshwater reservoirs: Scoping paper*
 1039 (IHP/GHG-WG/3; p. 28). UNESCO/IHA, International Hydropower Association -
 1040 International Hydrological Programme, Working Group on Greenhouse Gas Status of
 1041 Freshwater Reservoirs. <https://unesdoc.unesco.org/ark:/48223/pf0000181713>
- 1042 UNESCO/IHA. (2010). *GHG Measurement Guidelines for Freshwater Reservoirs* (p. 154).
 1043 UNESCO/IHA, International Hydropower Association.

Formatted: English (United States)

Formatted: English (United States)

Formatted: Norwegian (Bokmål)

- 1046 [https://www.hydropower.org/publications/ghg-measurement-guidelines-for-freshwater-](https://www.hydropower.org/publications/ghg-measurement-guidelines-for-freshwater-reservoirs)
1047 [reservoirs](https://www.hydropower.org/publications/ghg-measurement-guidelines-for-freshwater-reservoirs)
- 1048 Vachon, D., & Prairie, Y. T. (2013). The ecosystem size and shape dependence of gas transfer
1049 velocity versus wind speed relationships in lakes. *Canadian Journal of Fisheries and Aquatic*
1050 *Sciences*, 70(12), Article 12. <https://doi.org/10.1139/cjfas-2013-0241>
- 1051 Valiente, N., Eiler, A., Allesson, L., Andersen, T., Clayer, F., Crapart, C., Dörsch, P., Fontaine, L.,
1052 Heuschele, J., Vogt, R., Wei, J., de Wit, H. A., & Hessen, D. O. (2022). *Catchment properties*
1053 *as predictors of greenhouse gas concentrations across a gradient of boreal lakes.*
1054 *10(880619)*. <https://doi.org/10.3389/fenvs.2022.880619>
- 1055 [Valinia, S., Englund, G., Moldan, F., Futter, M. N., Köhler, S. J., Bishop, K., & Fölster, J. \(2014\).](https://doi.org/10.1111/gcb.12527)
1056 [Assessing anthropogenic impact on boreal lakes with historical fish species distribution data](https://doi.org/10.1111/gcb.12527)
1057 [and hydrogeochemical modeling. *Global Change Biology*, 20\(9\), 2752–2764.](https://doi.org/10.1111/gcb.12527)
1058 <https://doi.org/10.1111/gcb.12527>
- 1059 van Grinsven, S., Oswald, K., Wehrli, B., Jegge, C., Zopfi, J., Lehmann, M. F., & Schubert, C. J.
1060 (2021). Methane oxidation in the waters of a humic-rich boreal lake stimulated by
1061 photosynthesis, nitrite, Fe(III) and humics. *Biogeosciences*, 18(10), 3087–3101.
1062 <https://doi.org/10.5194/bg-18-3087-2021>
- 1063 Wanninkhof, R. (2014). Relationship between wind speed and gas exchange over the ocean revisited.
1064 *Limnology and Oceanography: Methods*, 12(6), Article 6.
1065 <https://doi.org/10.4319/lom.2014.12.351>
- 1066 Weiss R.F. & Price B.A. (1980) Nitrous oxide solubility in water and seawater. *Marine Chemistry*, 8,
1067 347-359. [https://doi.org/10.1016/0304-4203\(80\)90024-9](https://doi.org/10.1016/0304-4203(80)90024-9)
- 1068 [Weyhenmeyer, G. A., Hartmann, J., Hessen, D. O., Kopáček, J., Hejzlar, J., Jacquet, S., Hamilton, S.](https://doi.org/10.1038/s41598-019-46838-w)
1069 [K., Verburg, P., Leach, T. H., Schmid, M., Flaim, G., Nöges, T., Nöges, P., Wentzky, V. C.,](https://doi.org/10.1038/s41598-019-46838-w)
1070 [Rogora, M., Rusak, J. A., Kosten, S., Paterson, A. M., Teubner, K., ... Zechmeister, T.](https://doi.org/10.1038/s41598-019-46838-w)
1071 [\(2019\). Widespread diminishing anthropogenic effects on calcium in freshwaters. *Scientific*](https://doi.org/10.1038/s41598-019-46838-w)
1072 [Reports, 9\(1\), Article 1. <https://doi.org/10.1038/s41598-019-46838-w>](https://doi.org/10.1038/s41598-019-46838-w)
- 1073 Wilhelm E., Battino R. & Wilcock R.J. (1977) Low-pressure solubility of gases in liquid water.
1074 *Chemical Reviews*, 77, 219-262. <https://doi.org/10.1021/cr60306a003>
- 1075 Wilson J., Munizzi J. & Erhardt A.M. (2020) Preservation methods for the isotopic composition of
1076 dissolved carbon species in non-ideal conditions. *Rapid Communications in Mass*
1077 *Spectrometry*, 34. <https://doi.org/10.1002/rcm.8903>
- 1078 Xiao, S., Yang, H., Liu, D., Zhang, C., Lei, D., Wang, Y., Peng, F., Li, Y., Wang, C., Li, X., Wu, G.,
1079 & Liu, L. (2014). Gas transfer velocities of methane and carbon dioxide in a subtropical
1080 shallow pond. *Tellus B: Chemical and Physical Meteorology*, 66(1), 23795.
1081 <https://doi.org/10.3402/tellusb.v66.23795>
- 1082 Xu F.F. & Imlay J.A. (2012) Silver(I), Mercury(II), Cadmium(II), and Zinc(II) Target Exposed
1083 Enzymic Iron-Sulfur Clusters when They Toxify Escherichia coli. *Applied and Environmental*
1084 *Microbiology*, 78, 3614-3621. <https://doi.org/10.1128/aem.07368-11>
- 1085 Yamamoto S., Alcauskas J.B. & Crozier T.E. (1976) Solubility of methane in distilled water and
1086 seawater. *Journal of Chemical and Engineering Data*, 21, 78-80.
1087 <https://doi.org/10.1021/je60068a029>
- 1088 Yan, F., Sillanpää, M., Kang, S., Aho, K. S., Qu, B., Wei, D., Li, X., Li, C., & Raymond, P. A.
1089 (2018). Lakes on the Tibetan Plateau as Conduits of Greenhouse Gases to the Atmosphere.
1090 *Journal of Geophysical Research: Biogeosciences*, 123(7), 2091–2103.
1091 <https://doi.org/10.1029/2017JG004379>
- 1092 Yang H., Andersen T., Dorsch P., Tominaga K., Thrane J.E. & Hessen D.O. (2015) Greenhouse gas
1093 metabolism in Nordic boreal lakes. *Biogeochemistry*, 126, 211-225.
1094 <https://doi.org/10.1007/s10533-015-0154-8>

Formatted: Norwegian (Bokmål)